

# SoK: Analyzing Adversarial Examples: A Framework to Study Adversary Knowledge

Lucas Fenaux  
*University of Waterloo*  
*lucas.fenaux@uwaterloo.ca*

Florian Kerschbaum  
*University of Waterloo*  
*florian.kerschbaum@uwaterloo.ca*

## Abstract

Adversarial examples are malicious inputs to machine learning models that trigger a misclassification. This type of attack has been studied for close to a decade, and we find that there is a lack of study and formalization of adversary knowledge when mounting attacks. This has yielded a complex space of attack research with hard-to-compare threat models and attacks. We focus on the image classification domain and provide a theoretical framework to study adversary knowledge inspired by work in order theory. We present an adversarial example game, inspired by cryptographic games, to standardize attacks. We survey recent attacks in the image classification domain and classify their adversary’s knowledge in our framework. From this systematization, we compile results that both confirm existing beliefs about adversary knowledge, such as the potency of information about the attacked model as well as allow us to derive new conclusions on the difficulty associated with the white-box and transferable threat models, for example, that transferable attacks might not be as difficult as previously thought.

## 1 Introduction

Many machine learning (ML) models are currently deployed in critical environments like healthcare [1], self-driving cars [2], aerospace and aviation [3], and many more. Model failures in these settings can directly incur grave consequences on human life. While there exists a large body of literature on the safe and secure deployment of these models, the proposed solutions remain mainly academic, difficult to implement and replicate, and fall short of the security and safety standards we would typically expect from critical systems. Despite all of this, the deployment of ML models continues to grow. This surge in deployment, while promising, introduces a pressing concern: the vulnerability of these models to security flaws, both known and yet to be uncovered. The potential consequences of such vulnerabilities extend far beyond the limits of academia, with economic and societal implications.

Adversarial example attacks are one such attack, originally discovered by Szegedy et al. [4] in 2014. They have shown the existence of easily craftable imperceptible vulnerabilities in image classifiers. These vulnerabilities have taken the form of perturbations, imperceptible to the human eye, that can significantly alter a model’s prediction on an otherwise benign input. The low requirements for mounting adversarial attacks make it a prime vulnerability. Prior work in the domain of adversarial examples suggests a notable advantage for attackers, with the majority of attacks capable of, to some degree, impeding model performance. Among the existing defenses, few techniques have demonstrated a degree of robustness when it comes to safeguarding machine learning models, for example, adversarial training methods [5] and ensemble approaches [6] (and their combination). However, even in their strongest forms and under strict threat models that greatly limit the attacker’s capabilities, current defenses still fail to provide adequate protection. To remedy this, a branch of research on provably robust defenses emerged [7]. However, in practice, this is not yet a feasible approach since it increases the computational cost of model inference by several orders of magnitude. Since provable defenses are impractical, a majority of the field has focused on improving the quality of empirical defenses. Nevertheless, the absence of a reliable evaluation standard or assessment method for overall performance has resulted in an ongoing competitive cycle between attackers and defenders based on empirical experiments. A complete theoretical framework is necessary to create an evaluation standard and shift this competitive cycle into a manageable challenge for adversarial example research.

In our work, we focus on the image classification domain and aim to address a significant challenge: the current lack of emphasis on rigorous assessment of adversary knowledge in threat models. Adversary knowledge is one of the key components of a well-defined threat model and has long been overlooked and neglected by both attack and defense works. We study the current lack of formalization of adversary knowledge in adversarial example research and how it affects attack

comparability and performance. Defending against attackers with ill-defined capabilities places an additional burden on the defender. Whereas attacking with ill-defined knowledge hinders reproducibility and comparability. We develop this formalization as a theoretical framework to model various adversarial example attacks. We conduct a thorough review of recent attacks in the image classification domain, offering an up-to-date overview of the current landscape of adversaries in this specific context [8–90]. This formalization allows us to define and categorize attacks and their associated threat models, in turn, laying a foundation for defenses. Additionally, combined with our survey of attacks, we measure the effect of the information available to an attacker on an attack’s performance. We compare various threat models and confirm, with falsifiable results, the generally held belief that certain categories of information, like information related to the attacked classification model, have a disproportionate effect on attack performance. However, we also find that a lack of information in that category, in the case of transferable attacks, can be compensated by the use of additional information such as information related to the training data or the training process, to yield attacks that are almost as potent.

## 2 Definitions

We let  $I \subset \mathbb{R}^*$  be the set of all possible inputs,  $\mathcal{L} \subset \mathbb{R}^* \cup \{\perp\}$  the set of all possible labels, and the ground-truth function  $gt : I \rightarrow \mathcal{L}$  as the function that assigns its true label to an input sample.

**Definition 1** (Adversarial Example). *An input sample  $i \in I$  and its associated label  $gt(i) \in \mathcal{L}$  is said to be adversarial if it was specifically crafted to successfully trigger a learned model to output an incorrect answer.*

**Definition 2** (Grounded Adversarial Example). *An input sample  $i \in I$  and its associated label  $gt(i) \in \mathcal{L}$  is said to be a grounded adversarial example if it was created using a benign sample  $x \in I$  and its associated label  $gt(x) \in \mathcal{L}$ .*

**Definition 3** (Targeted/Untargeted Adversarial Example). *An input sample  $i \in I$  and its associated label  $gt(i) \in \mathcal{L}$  is said to be a targeted adversarial example if for a fixed chosen label  $c \in \mathcal{L}, c \neq gt(i)$ , it triggers a learned model to output label  $c$ . However, if it triggers a learned model to output a label  $l \neq gt(i), l \in \mathcal{L}$ , we say it is untargeted.*

## 3 Previous Work

We formalize adversarial example attacks with an emphasis on the information and the capabilities the adversary has access to perform their attack. There has been a lack of a proper theoretical framework that is based on proper security principles. In turn, this has been reflected in work whose

impact is limited due to the inherent flaws in their security assumptions.

Previous systematization of knowledge works [91, 92] have looked at the adversarial example problem from various angles. Papernot et al. [91] took a holistic approach and proposed a thorough overview of the possible threat models as well as the training and inference process in an adversarial setting. They emphasized a clear distinction between the different domains (physical vs. digital) while describing the overall ML attack surface. This was reiterated more recently by Lin et al. [59] where the authors present an attack on the physical domain specifically. In contrast, Byun et al. [42] took advantage of the properties of the physical domain by projecting adversarial examples onto virtually 3D-rendered physical objects (like a mug) to improve the transferability of their attack. Another approach was the one by Carlini & Wagner [92]. In their paper, they present generating adversarial examples as a constrained optimization problem. They first cover a set of existing attacks at the time and from their formalization, they introduced three new attacks adapted each for a specific norm distance metric ( $L_0$ -norm,  $L_1$ -norm, and  $L_2$ -norm). However, we found that these works fail to properly cover adversarial information and capabilities. This was not a significant problem back in 2017 and 2018 when most of the literature focused on white-box attacks, attacks where the adversary has immense knowledge and capabilities and therefore covering the minutia is not as important.

Recently, however, the field has experienced a shift toward more realistic and usable attacks. This is reflected in the emergence of unrestricted adversarial examples [82, 83, 93] as well as threat models like the black-box and no-box (transferable) threat models [8, 42, 51, 78, 80, 89]. A work that took the first step toward rationalizing this shift is the work of Gilmer et al. [94]. One of the core messages of their work is that, at the time, research on adversarial examples was predominantly focused on abstract, hypothetical scenarios that lacked direct relevance to any specific security issues. This still partially holds up to this day. They did mention the question of the attacker’s knowledge but did not go into depth beyond the already common concepts of white-box and black-box. Papers on defense techniques have also not provided a comprehensive account of attackers’ capabilities and constraints that would be applicable in real-world security scenarios. However, they presented a wide-reaching list of salient situations that represent at their core the action space of the attacker. The action space of an attacker can be defined as the set of potential actions or strategies at the disposal of an adversary. This encompasses the various methods and choices available to the attacker when attempting to compromise a system, exploit vulnerabilities, or achieve their malicious goals during an attack.

In this work, we propose to delve deeper into the knowl-

edge that an attacker has when performing an attack. This goes beyond the knowledge of the machine learning system that they are trying to attack. It includes access to data and computing resources, as well as knowledge of the code and hyperparameters used to set up and train said machine learning system.

## 4 Formalization

A key element to differentiate between inference time attacks is the action space that is available to the attacker. Real-world practical restrictions are translated into mathematical constraints on the generated adversarial examples. Gilmer et al. [94] first define the action space of the adversary for adversarial example attacks. In their paper, they identify five salient situations: indistinguishable perturbations, content-preserving perturbations, non-suspicious input, content-constrained input and unconstrained input. Historically, adversarial example attacks have been studied under the indistinguishable and content-preserving perturbation settings, but recently have been extended to the non-suspicious and content-constrained input settings.

To propose a unified theoretical framework that can accommodate every salient situation, we introduce an object that is already well-defined in the field of cryptography: the distinguisher.

Our fundamental challenge is rooted in simulating human-like image perception, a problem lacking a well-established mathematical framework. Consequently, we must define our own setting, complete with its corresponding distinguisher. The context we are operating within assumes human-like capabilities for the distinguisher, for example, for indistinguishable perturbations, it is so human reviewers would not be able to distinguish that the image is adversarial. Therefore, we need to introduce a new class of distinguishers, the **human-like distinguisher** that we define as a distinguisher whose capabilities match that of a human or any human-made real-world system. Current existing metrics ( $l_p$ -norm, similarity, quality...) all fall under this category and are used as an approximation of human-like capabilities for their salient situation.

We can now represent a salient situation as a distinguisher  $D : I \rightarrow \{0, 1\}$  who attempts to output 0 on benign samples and 1 on adversarial samples, it is meant to capture the detection capabilities in place in the system under attack. We can use this formalization of salient situations and provide a proper formalization of the notion of *indistinguishability* for any setting, not just the indistinguishable perturbation setting.

**Definition 4** (Indistinguishability). *Assuming a salient situation with distinguisher  $D : I \rightarrow \{0, 1\}$ , let  $A, B \subset I$  where  $A$  is the set of all adversarial examples and  $B$  is the set of all benign samples, we say an input  $x \in I$  is indistinguishable if we have:*

$$\zeta(n) = \left| \Pr_{x \leftarrow A} [D(x) = 1] - \Pr_{x \leftarrow B} [D(x) = 1] \right| = 0 \quad (1)$$

However, this definition is too restrictive as in practice  $n$  (and therefore the number of possible adversarial examples) is too large to obtain  $\zeta(n) = 0$  and should only serve as a target for the community to strive for rather than a strict requirement. Instead, for practical purposes, we can use a loosened notion of *stealth* to bind adversarial examples.

**Definition 5** (Stealth). *If  $\zeta(n)$  (from Equation 4) is  $\zeta(n) \in O(\frac{\log(n)}{n})$ ,  $|A \cup B| = n$ , then we say that the associated input  $x \in I$  is stealthy.*

### 4.1 Categorization

#### 4.1.1 Information Extraction Oracles

To formalize the information an adversary has access to when performing an attack, we need a generic representation of information. Since precisely quantifying and defining information is quite difficult, we avoid it and instead present a generic method for representing information acquired by the adversary. To that effect, we introduce Information Extraction Oracles (IEOs). IEOs serve as a translation tool that allows an attacker to properly defined information in a threat model. They can be used to represent the access to information available to the attacker (through any of its attack capabilities). We now introduce an improved method for presenting threat models in a standardized and formalized fashion.

**Definition 6** (Information Extraction Oracle). *An Information Extraction Oracle  $O : \{0, 1\}^* \rightarrow \{0, 1\}^*$  is a stateful oracle machine that can take in a query and outputs information in a binary format.*

We define the set of all information extraction oracles as  $\mathbb{O}$ . Instead of describing attacker capabilities with vague terminology, we can now use information extraction oracles to precisely and accurately capture the attacker’s knowledge and capabilities. As mentioned in Definition 6, information extraction oracles are stateful. The adversary can extract the oracle’s state using the *State* function.

**Definition 7.** *We define the function  $State : \mathbb{O} \rightarrow \mathbb{R}^*$  that takes in as input an Information Extraction Oracle and outputs its current state as a set of real numbers. If the input oracle does not have a state, it returns  $\emptyset$ .*

To accurately represent relationships between various threat models (white-box vs. black-box for example), we need to introduce a relational structure to information extraction oracles. To do so, we define the domination  $\sqsupseteq$  operator on IEOs.

We define the different symbols we use:

- $\{\}$  represents an unordered set
- $\square$  represents an ordered set
- $\cdot$  represents what we call an element, which we define as anything that is not a set.

**Definition 8** (Information Extraction Oracle domination operator). We define the operator  $\sqsubset$  for information extraction oracles over their outputs in the following way:

Let  $O_1(a) = x$  and  $O_2(a) = y$ . We have three base cases:

- (a)  $x$  and  $y$  are both sets. Then  $O_2 \sqsubset O_1$  if  $\forall a \in I, x \subset y$ .
  - (b)  $x$  is an element and  $y$  is an unordered set. Then  $O_2 \sqsubset O_1$  if  $\forall a \in I, x \in y$ .
  - (c)  $x$  is either an unordered set or an element and  $y$  is an element. Then  $O_2 \sqsubset O_1$  if there exists a probabilistic polynomial-time (PPT) function  $f$  s.t.  $\forall a \in I, f(x) = y$ .
- Using these base cases, we can expand to the three ordered set cases.
- (a)  $x = [x_1, \dots, x_n]$  is an ordered set and  $y$  is either an unordered set or an element ( $n$  is a positive integer). Then  $O_2 \sqsubset O_1$  if  $(y \sqsubset x_1) \vee \dots \vee (y \sqsubset x_n)$ .
  - (b)  $x$  is an unordered set or an element and  $y = [y_1, \dots, y_k]$  is an ordered set ( $k$  is a positive integer). Then  $O_2 \sqsubset O_1$  if  $(y_1 \sqsubset x) \wedge \dots \wedge (y_k \sqsubset x)$ .
  - (c)  $x = [x_1, \dots, x_n]$  is an ordered set and  $y = [y_1, \dots, y_k]$  is an ordered set ( $n$  and  $k$  are positive integers). Then  $O_2 \sqsubset O_1$  if  $\forall i \in \{1, \dots, k\}, \exists j \in \{1, \dots, n\}$  s.t.  $y_i \sqsubset x_j$ .

We let  $\not\sqsubset$  be the not operator for  $\sqsubset$ . Meaning when not  $A \sqsubset B$ , then  $A \not\sqsubset B$ .

When an attacker has access to multiple oracles  $O_A, O_B$  where a domination relation cannot be established, we describe the resulting combined oracle in Definition 9.

**Definition 9** (Information Extraction Oracle Combination). Given two IEOs  $O_A, O_B$  for which neither  $O_A \sqsubset O_B$  nor  $O_B \sqsubset O_A$  is true. Then we define the combined oracle  $O_{A\&B}$  as follows:  $O_{A\&B}(x) = [O_A(x), O_B(x)]$

### 4.1.2 Information Categories

An IEO provides an interface for the attacker to both the knowledge of the defender (for example, information about the target model) and any additional external knowledge possessed by the attacker (for example, an additional dataset that is disjoint from the defender’s training set but is drawn from the same distribution). We can then categorize the different aspects of a threat model into different IEOs that allow the attacker access to the associated information. We used all the threat models we observed in the literature to build this categorization to have a complete representation of the threat models in the field and a meaningful categorization.

We can classify the information involved in an adversarial example attack into three distinct types: information **used**

by the defender, **generated** by the defender (for example model parameters  $\theta_M$ ) and any information that is **publicly accessible** (data, pre-trained models ...).

Within those classes, we identified the salient categories that combined can be used to reconstruct any threat model: **model, data, training** and **defense** information.

### 4.1.3 Information Hasse Diagrams

Now that we have defined broad information categories for attackers, we can introduce a structure that will allow for meaningful comparisons between sets of assumptions within each category.

We make use of the  $\sqsubset$  operator that we defined in Definition 8 to build Hasse diagrams. These diagrams are usually used to visually represent sets ordered by inclusion. We design our Hasse Diagrams to visually represent our oracles ordered by  $\sqsubset$ . For each category, we provide the associated Hasse diagram. In order theory, a Hasse diagram is supposed to represent finite partially ordered sets, however, we extend it to infinite partially ordered sets by allowing formulaic set descriptions (which can expand to generate infinite but partially ordered sets). For simplicity’s sake, when we describe information extraction oracles, we assume that the inputs they are queried with are in  $I$  (in the image domain), otherwise, they return an empty ordered set  $\square$ . We summarize all the behavior of the information extraction oracles we define in Table 1.

#### Model information Hasse diagram:

For model-related information, it can either be *static* or *query-based*. For static information, we have:

- Model parameters  $\theta_M$  (white-box). Let  $O_M$  be its information extraction oracle.
- Model architecture: either the exact model architecture or a set of possible architectures.
  - Exact model architecture  $\phi_M$ . Let  $O_A$  be its information extraction oracle.
  - Set of possible architectures: Let  $O_{SPA}$  be its information extraction oracle.

For query-based information, we have:

- Query-access to model scores (model logit probabilities or values on queried inputs). Let  $O_S$  be its information extraction oracle.
- Query-access to model labels (predicted class on queried inputs). Let  $O_L$  be its information extraction oracle.

We can then order their associated information extraction oracles in a Hasse Diagram in Figure 1.

**Theorem 1.** Figure 1 holds under the  $\sqsubset$  ordering.

We refer to Appendix A for all of the proofs.

**Data Information Hasse Diagram** We identify three sets of data. The training data  $\mathcal{D} \subset I \times \mathcal{L}$  that was used to train



Oracle	Output	State
$O_M$	$[\theta_M, x]$	$\square$
$O_S$	$[M(x), x]$	number of queries left $[k]$
$O_L$	$[\text{argmax}(M(x)), x]$	number of queries left $[k]$
$O_A$	$[\phi_M, x]$	$\square$
$O_{SPA}$	$[\{\phi_0, \phi_1, \dots, \phi_k\}, x]$ , $k \in \mathbb{Z}^+$ and for some $i \sim \mathcal{U}(0, k), \phi_i = \phi_M$	$\square$
$O_{\mathcal{D}}$	$[\mathcal{D}, x]$	$\square$
$O_{\mathcal{D}'}$	$[\mathcal{D}', x]$	$\square$
$O_{\mathcal{E}}$	$[\mathcal{E}, x]$	$\square$
$O_{Train}$	$[Train, x]$	$\square$
$O_{T_i}$	$[T_i, x]$	$\square$
$O_{FA}$	$[\rho, \varrho, x]$	$\square$
$O_{PA}$	$[\rho, \{\varrho_1, \dots, \varrho_k\}, x]$ , $k \in \mathbb{Z}^+$ and for some $i \sim \mathcal{U}(0, k), \varrho_i = \varrho$	$\square$
$O_{SPD}$	$[\{\rho_0, \dots, \rho_k\}, \{\varrho_1, \dots, \varrho_k\}, x]$ , $k \in \mathbb{Z}^+$ and for some $i \sim \mathcal{U}(0, k), \rho_i = \rho$ and $\varrho_i = \varrho$	$\square$

Table 1: Oracle Table

the target model  $M$  and its information extraction oracle  $O_{\mathcal{D}}$ . Any other data samples  $\mathcal{D}' \subset I \times \mathcal{L}$  (and it's IEO  $O_{\mathcal{D}'}$ ) that were drawn from the same distribution as  $\mathcal{D}$  but were not in the training data. Finally, any other data samples  $\mathcal{E} \subset I \times \mathcal{L}$  (and it's IEO  $O_{\mathcal{E}}$ ) that were not drawn from the same distribution as  $\mathcal{D}$  and  $\mathcal{D}'$ . In this case, creating the Hasse diagram is relatively straightforward because we only need to contemplate all feasible power set combinations of oracles using definition 9.

**Theorem 2.** *Figure 2 holds under the  $\square$  ordering.*

**Training Information Hasse Diagram** We describe a systematized method for identifying a training function's known elements. First, we must define exactly what we mean by training algorithm or function.

**Definition 10** (Train function). *We define a training function  $Train : \{0, 1\}^* \rightarrow \mathcal{M}$  as the function representing the algorithm used by the defender to generate the target model  $M$ .*

The  $Train$  function takes in the algorithm's hyperparameters as well as any other information needed to train the model. We can articulate known information about the training algorithm as one of the following training information sets:

$\overline{T} = \{Train' | g_{Train}(Train') = True\}$  where  $g_{Train}$  is a function that returns  $True$  if a particular condition in the training

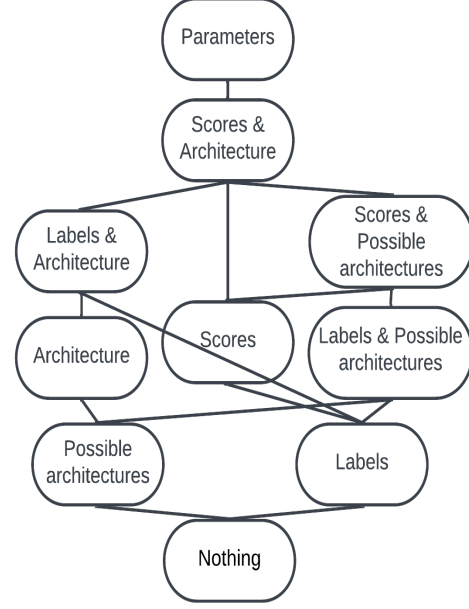


Figure 1: Model Oracle Hasse Diagram

algorithm with respect to the original  $Train$  function is satisfied (e.g. the training algorithm uses cross-entropy loss) and  $False$  otherwise. We can then create two types of information extraction oracles. This is the information that can be used (combined with data) to train/assume access to pre-trained models. The first one is  $O_{Train}$ , where  $Train$  is the original  $Train$  function used by the defender.

The other is when the attacker has access to one of the sets  $T$ . There are infinitely many of them, therefore we will just define a generic oracle for them:  $O_{T_i}$  for any integer  $i$  where  $T_i$  is any one of the sets  $T_i = \{Train' | g_{Train}^i(Train') = True\}$  we previously described.

The oracles generated from this generic oracle can then be ordered using  $\square$  following the usual rules defined in Definition 8.

**Theorem 3.** *Figure 3 holds under the  $\square$  ordering.*

**Defense Information Hasse Diagram** Defense information is any defense mechanisms put in place by the defender on top of the distinguisher  $D$ . We can partition it as follows:

- **Full awareness** of the defense and its parameters (similar to white-box for model information). We represent this as an algorithm  $\rho$  and its parameters  $\varrho$ . Let  $O_{FA}$  be its information extraction oracle.
- **Partial awareness** of the defense and its parameters: knowledge of the defense  $\rho$  but not the specific parameters of the instance. Let  $O_{PA}$  be its information extraction oracle.
- A set of potential defenses that can be obtained by having partial insider information. Let  $O_{SPD}$  be its informa-

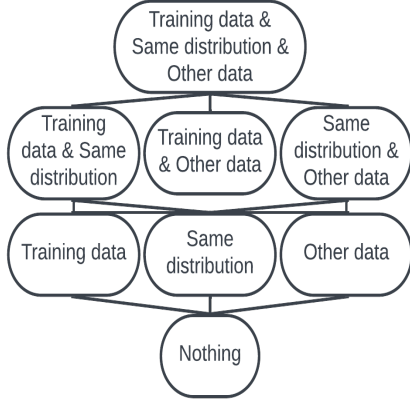


Figure 2: Data Oracle Hasse Diagram



Figure 4: Defense Oracle Hasse Diagram

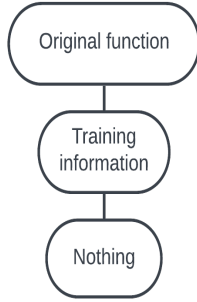


Figure 3: Train Oracle Hasse Diagram

tion extraction oracle.

**Theorem 4.** *Figure 4 holds under the  $\sqsubseteq$  ordering.*

## 4.2 Adversarial Example Game

Gilmer et al. [94] were also among the first to present the problem of adversarial examples as a security game. This contrasts with Carlini & Wagner [92] and their optimization-based representation. This emphasized the security nature of the problem. They also address in their paper the notion of game sequence. It is the player order and whether the game is repeated. This was not particularly addressed by Carlini & Wagner [92] but is key to a practical understanding of the problem. It relates the problem of adversarial examples to those of standard cryptographic security games. Later, Bose et al. [88] expanded upon the game nature of adversarial examples while relating it to its underlying min-max optimization nature. They use this expansion to develop an attack in what they call the NoBox (also called transferable) setting and to bridge the gap between the theory and the empirical in more demanding and realistic threat models. We present an updated, concise and comprehensive security game for adversarial examples that conforms with the security and machine learning communities.

### 4.2.1 Definitions

First, we define the following:  $\emptyset$  is the termination symbol.  $O_X^{a,b}$  is an input information extraction oracle about the data granted to the adversary for an attack. We superscript  $O_X^{a,b}$  with a bit  $a$  that represents whether the attack is grounded or not (0 for grounded and 1 for not-grounded). We also superscript it with a bit  $b \in \{0, 1\}$  where if the attack is untargeted then  $b = 0$  and if it is targeted then  $b = 1$ . It returns the start input sample  $x \in I$  and its associated ground-truth label  $y \in \mathcal{L}$  if the attack is grounded. In the case of a targeted attack, it also returns the target label  $y_t \in \mathcal{L}$ .  $O_{Dist}$  is an information extraction oracle that returns a distinguisher  $D'$  that the attacker can utilize to verify that the generated adversarial examples are within the restrictions of the salient situation. By default,  $D' = D$  where  $D$  is the actual distinguisher used by the defender. However, in situations where only partial information is known about the distinguisher  $D$  or the associated salient situation,  $D'$  can be used to capture the attacker's knowledge of  $D$ .

We can now define the key functions that we will use in our security game:

**Definition 11 (AdvGen).**  $AdvGen : \mathbb{O} \rightarrow I \times \mathcal{L}$ .  $AdvGen(O)$  on input set of information oracles  $O \subset \mathbb{O}$  (including the input information oracle  $O_X^{a,b}$ ), outputs the following:

$$AdvGen(O) = [x', y'] \quad (2)$$

where  $x' \in I$  is the adversarial example and  $y' \in \mathcal{L}$  is its ground-truth label.

Additionally, we also define two other functions that are vital to our security game: *Evaluate* and *Classify*. As mentioned in Gilmer et al.'s work [94], an attacker can have different goals, therefore we use the *Evaluate* function to represent an attack's success with respect to the attacker's goal. (Either a targeted or an untargeted (Definition 3) attack or any other goal an attacker might have).

**Definition 12** (*Classify*).  $\text{Classify}(M, x)$  on input model  $M$  and input sample  $x \in I$  returns the predicted label of  $x$  using the classifier  $M$  while executing any inference-time pre-processing or defense mechanisms the defender has in place.

**Definition 13** (*Evaluate*). We have two evaluation functions, one for untargeted attacks  $\text{Evaluate}_0$  and one for targeted attacks  $\text{Evaluate}_1$  (same as  $\mathcal{O}_X^{a,0}$  and  $\mathcal{O}_X^{a,1}$ ). They are defined as the following:

$$\text{Evaluate}_0(y, r) = \mathbb{I}[r \neq y] \quad (3)$$

and

$$\text{Evaluate}_1(y_t, r) = \mathbb{I}[r = y_t] \quad (4)$$

Where  $y$  is the ground-truth label,  $r$  is the predicted label and  $y_t$  is the target label for a targeted attack.

Now that we have all the components of the game ready, we can define it in Figure 5. This game has two participants, the attacker and the defender.

#### 4.2.2 Measuring Success

First, we have to define success before being able to measure it. We define success as our game returning 1 and failure as our game returning 0. This definition guarantees that the attacker succeeds if and only if he manages to remain undetected by the defender while completing his objective (usually misclassification). Let  $G(O, D', \text{Evaluate}_b, D, \text{Train}, \text{Classify}) \rightarrow \{0, 1\}$  be an instance of the game. What is currently used to measure success is the following:

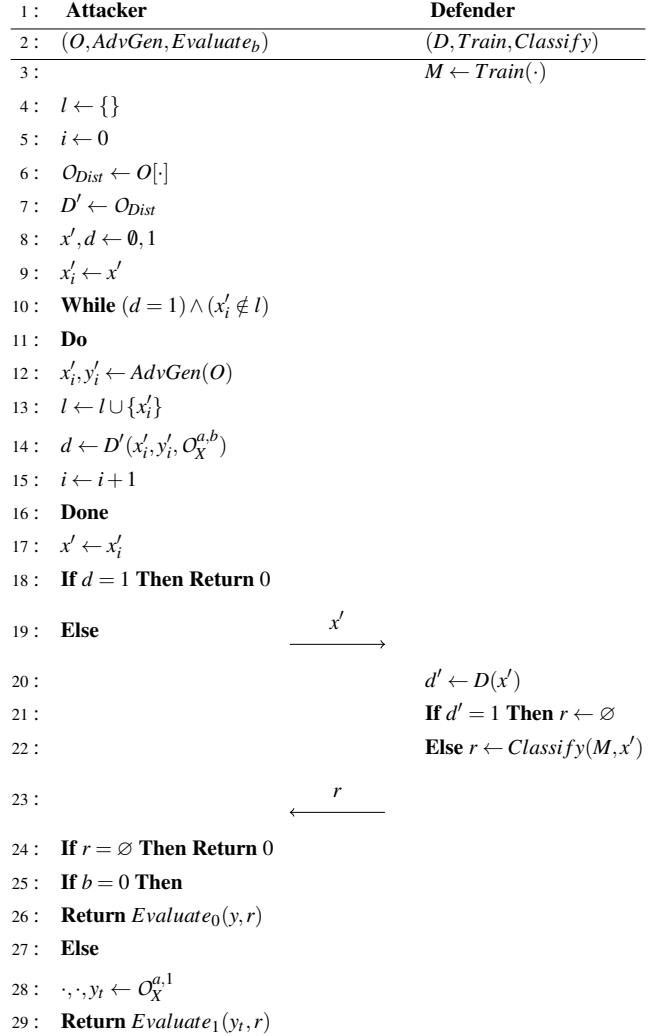
**Definition 14** (Expected success rate). We define the expected success rate (ESR) as:

$$\xi_G = \mathbb{E}[G(O, D', \text{Evaluate}_b, D, \text{Train}, \text{Classify})] \quad (5)$$

It is also known as Attack Success Rate (ASR). However, it can be deceiving as it rewards attacking already poorly performing models and, without additional information, can misrepresent an attack's performance. Let  $G_b(O_X, \text{Evaluate}_b, D, \text{Train}, \text{Classify})$  be the version of our game where instead of being given adversarial examples, the defender is provided with benign samples. We use the expected success rate on this game  $\Upsilon_{G_b}$  as a lower-bound for attack performance. For simplicity's sake, we write  $G(O, D', \text{Evaluate}_b, D, \text{Train}, \text{Classify})$  as  $G$  and  $G_b(O_X, \text{Evaluate}_b, D, \text{Train}, \text{Classify})$  as  $G_b$ . We instead propose the following score as an alternative performance measurement.

**Definition 15** (Relative performance score). We define the relative performance score as:

$$\Upsilon_{G, G_b} = \xi_G^2 - \xi_{G_b}^2 \quad (6)$$



← is the assignment operator. = is the equality comparison operator. · is used as a placeholder for an index.

Figure 5: Adversarial Example Game Diagram Algorithm

This score is contained between  $-1$  and  $1$ . This relative score alleviates the aforementioned problem. The score is negative when the attack performs worse than just using benign samples and is positive otherwise. We believe it captures the various trade-offs when mounting attacks and defenses more fairly than the expected success rate or even a shifted expected success rate by the lower-bound ( $G_b$ ). Figure 6 provides a visual understanding of the behavior of this score when varying both  $\xi_G$  and  $\xi_{G_b}$ .

#### 4.2.3 Example: PGD

We will now showcase an application of our formalization to an existing well-known and well-performing attack: Projected Gradient Descent (PGD) [5]. This should function as

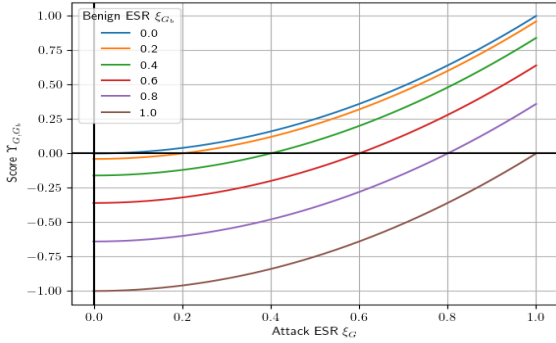


Figure 6: Relative Performance Score for various benign and adversary ESRs.

a template for the practical application of our formalization and the associated game. As a reminder, the multistep PGD attack can be defined as the following:

$$x^{t+1} = \Pi_{x+\mathcal{S}}(x^t + \alpha \text{sgn}(\nabla_x L(\theta, x, y))) \quad (7)$$

where  $x$  is the original benign sample with its label  $y$ ,  $x^t$  is the input at step  $t$  of the attack,  $\mathcal{S} \subseteq \mathbb{R}^d$  is the set of allowed perturbations ( $d$  is the input dimension),  $\theta$  are the model parameters,  $L$  is a loss function,  $\text{sgn}$  is the sign function (-1 if input is negative, 1 otherwise) and  $\alpha$  is the step size. In their paper, they consider the following adversaries:

1. "White-box attacks with PGD for a different number of iterations and restarts, denoted by source  $A$ ".
2. "White-box attacks with PGD using the Carlini-Wagner (CW) loss function (directly optimizing the difference between correct and incorrect logits)".
3. "Black-box attacks from an independently trained copy of the network, denoted  $A'$ ".
4. "Black-box attacks from a version of the same network trained only on natural examples, denoted  $A_{nat}$ ".
5. "Black-box attacks from a different convolution architecture, denoted  $B$ ".

Table 2 summarizes the adversary knowledge used in each version.

Our knowledge tables allow for a clear and concise representation of the adversary’s knowledge of the defender’s information. We will then describe the components of the game for the first adversary (Attack #1). This is meant as a template to showcase how one would describe their attack using our game. To do this, we need to define the following components:  $O$ ,  $D$ ,  $D'$ ,  $Evaluate_b$ ,  $Classify$ ,  $Train$ , and  $AdvGen$ .

As shown in Table 2, we have the associated oracles used by the attacker in Attack #1 that are the following:  $O = \{O_M, O_{T_1}, O_{FA}, O_X^{0,0}, O_{Dist}\}$ . For the training information (loss function) of Attack # 1, we construct  $O_{T_1}$ , we let

Attack	Model	Data	Train	Defense
1	Parameters	$\emptyset$	Training Information (loss function)	$\emptyset$
2	Parameters	$\emptyset$	$\emptyset$	Full Awareness
3	Scores & Architecture	Training Data	Original Function	Full Awareness
4	Scores & Architecture	Training Data	Original Function	$\emptyset$
5	Possible Architectures	Training Data	Original Function	Full Awareness

Table 2: PGD attacks knowledge table

$T_1 = \{Train' | g_{Train}^1(Train') = True\}$  where  $g_{Train}^1$  is the function that returns True when  $Train'$  uses the same loss function as  $Train$ .

$D$  varies depending on the dataset used, for example, on MNIST [95], they use an *indistinguishable-perturbation* distinguisher with the  $l_\infty$ -norm metric and a maximum allowed perturbation of  $\epsilon = 0.3$  (for pixel values between 0 and 1). However, for CIFAR-10 [96], they also use an *indistinguishable-perturbation* distinguisher with the  $l_\infty$ -norm metric, but they use a maximum allowed perturbation of  $\epsilon = 8$  (for RGB pixel values between 0 and 255). They also explore a variant of their attack in the case of an  $l_2$ -bounded adversary but to keep this concise we do not analyze it.  $O_{Disc}(x) = D' = D$  for any  $x \in \{0, 1\}$  as it is assumed that the attacker knows exactly the setting it is in.

Their defense is part of the training process (adversarial training), therefore  $Classify(M, x) = M(x)$ . The adversary’s goal is to modify the attacked model’s accuracy, meaning it is an untargeted attack. Hence,  $b = 0$  and  $Evaluate_0(y, r) = \mathbb{I}(r \neq y)$ .  $Train$  (as defined) is the algorithm/code used to train the attacked model, due to the sheer complexity of the algorithm, we will instead point out that they link their code in their paper [5]. We can summarize it as a standard Stochastic Gradient Descent (SGD) based model training algorithm that incorporates adversarial training as a defense. Finally, for the adversarial example generation, they use a grounded process, hence  $a = 0$  and  $AdvGen$  can be defined as the algorithm described in Figure 7 (they have three hyperparameters  $t$ ,  $\alpha$ ,  $\epsilon$ ).

## 5 Survey Summary & Methodology

In Tables 3 and 15 in Appendix B, we summarize the findings of our survey by reporting the information used by each attack in the surveyed papers as well as the metric used to craft the adversarial examples. In the case where papers evaluate their attacks under multiple scenarios, we split the attack into multiple variants lettered (A), (B), and so on.



```

1:  $AdvGen(O)$   $t, \alpha, \epsilon$ 


---


2:  $O_M, O_{Train}, O_{FA}, O_X^{0,0}, O_{Dist} \leftarrow O$ 
3:  $i \leftarrow 0$ 
4:  $x, y \leftarrow O_X^{0,0}(0)$ 
5:  $\theta_M \leftarrow O_M(0)$ 
6:  $\dots, L, \dots \leftarrow O_{Train}(0)$ 
7:  $x^i \leftarrow x$ 
8: While  $i < t$ 
9: Do
10:  $x^{i+1} \leftarrow \Pi_{x+S}(x^i + \alpha \operatorname{sgn}(\nabla_x L(\theta_M, x, y)))$ 
11:  $x^{i+1} \leftarrow \operatorname{clip}(x^{i+1}, x - \epsilon, x + \epsilon)$ 
12:  $x^{i+1} \leftarrow \operatorname{clip}(x^{i+1}, 0, 1)$ 
13:  $i \leftarrow i + 1$ 
14: Done
15: Return  $x^i$ 

```

Figure 7: PGD Attack Algorithm

We focus on recent papers, papers published in 2022 or after to narrow the field of the search and allow for an up-to-date perspective of the field of image classification adversarial research. We gathered a total of eighty-three papers [8–90], that we then narrowed to twenty using quality and relevance [8, 11, 12, 34–37, 42, 51, 61, 62, 78–83, 88–90]. None of the papers gathered used any defense information (as it is more relevant to adaptive attacks) so we exclude it from Table 3. Table 3 contains only the papers included in the evaluation (Section 6). For the rest, we refer to Table 15 in Appendix B.

## 6 Evaluation

For this work, we focus our evaluation on indistinguishable perturbation untargeted attacks that were evaluated on the ImageNet [97] and CIFAR-10 [96] datasets, as these are the most studied datasets in the attacks we surveyed. To compare attacks, we only compare evaluations within datasets and we only work with results presented by the authors themselves in their papers. We first, if possible, compare papers against models that are from the exact same source (public provider). If that’s not possible, we compare models of the same architecture while also looking at their benign accuracies. In the case where a paper does not provide benign accuracies, we use the benign accuracy from another paper but report the result in *italics* to show its unreliability.

### 6.1 Attacks on the ImageNet dataset

First, we tackle the most evaluated dataset that we study in our work, with eleven variants of attacks evaluated against it: ImageNet [97]. We perform four comparisons in total. We

Attack (Targeted)	Model	Data	Train	Metric
LGV (A) [51]	Possible Architectures	Training Data	Training Function	$l_\infty$
LGV (B) [51]	Parameters	$\emptyset$	$\emptyset$	$l_\infty$
Pixle [34] (both)	Scores	$\emptyset$	$\emptyset$	$l_0$
MASSA [62]	Labels	$\emptyset$	$\emptyset$	$l_2$
SSAH (A) [61] (both)	Parameters	Same Distribution	$\emptyset$	$l_\infty$
SSAH (B) [61] (both)	Possible Architectures	Other Data	Training Function	$l_\infty$
BIA (A) [8]	Possible Architectures	Other Data	Training Function	$l_\infty$
BIA (B) [8]	Possible Architectures	Training Data	Training Function	$l_\infty$
BIA (C) [8]	Parameters	Training Data	$\emptyset$	$l_\infty$
ACG [79]	Parameters	$\emptyset$	Loss Function	$l_\infty$
ATA (A) [78]	Possible Architectures	Training Data	Training Function	$l_0$
ATA (B) [78]	Parameters	$\emptyset$	$\emptyset$	$l_0$
AEG (A) [88]	Architecture	Same Distribution	Loss Function & Optimizer	$l_\infty$
AEG (B) [88]	Possible Architectures	Training Data	Loss Function & Optimizer	$l_\infty$
A <sup>3</sup> [36]	Parameters	Same Distribution	Loss Function	$l_\infty$

Table 3: Attack Summary Table. We provide the information used by the attacker for each of the categories and the metric used to craft the adversarial examples.

summarize the results of our comparisons on ImageNet in Table 4. The only paper to evaluate their attack on defended models is ACG [79] where they get an average ESR of 68.50% and an average score of 0.314.

The takeaways for ImageNet are the following:

- Only query-based access to the model and no other information is sufficient to reduce an undefended model’s accuracy to almost 0%.
- Transferable settings can achieve extremely high ESRs (93.48% for BIA (B)), which shows that, at least in the undefended case, transferable attacks that use additional data and training information (usually to train surrogates) can achieve ESRs close to query-based and white-box

Model Information	Data Information	Training Information	Attack Variant	Und. ESR	Und. Score
Possible Architectures	Training Data	Training Function	LGV (A)	72.4	0.497
			BIA (B)	93.48	0.811
			ATA (A)	79.65	0.524
	Training Data & Same Distribution	Training Function	SSAH (B)	19.14	N/A
Labels	$\emptyset$	$\emptyset$	MASSA	99.49	0.916
Scores	$\emptyset$	$\emptyset$	Pixel	98.5	0.897
Parameters	Training Data	$\emptyset$	BIA (C)	97.82	0.883
	Same Distribution	$\emptyset$	SSAH (A)	95.56	0.915
		$\emptyset$	LGV (B)	97.1	0.885
		$\emptyset$	ATA (B)	100.0	N/A
		Loss Function	ACG	N/A	N/A

Table 4: ImageNet information and attack results. "Und." stands for undefended.

attacks. Unfortunately, since none of the transferable attacks we studied evaluated defended models, we cannot say if this extends to defended models.

- ImageNet-defended models are mostly broken by white-box attacks. ACG obtains an average ESR of 68.5% and an average score 0.314. While, defended models do perform better than undefended ones, the accuracy loss is still significant.

### 6.1.1 LGV (A) & BIA (B) & ATA (A) & SSAH (B)

We start by comparing the different transferable attacks: LGV (A) [51], BIA (B) [8], ATA (A) [78], SSAH (B) [61]. All these attacks attack undefended papers. Some share architectures, however, not all of them provide benign accuracies for the models they evaluate. We compile the results in Tables 5. BIA (B), LGV(A), and SSAH (B) both use the  $l_\infty$ -norm but BIA (B) uses a perturbation budget of 10/256 whereas SSAH (B) uses one of 8/256. LGV (A) does not specify the budget used. ATA (A) uses the  $l_0$ -norm, where they are only allowed to fully modify 1024 pixels. Unfortunately, this means that the following comparison is disparate.

BIA (B) outperforms the other attacks. Due to the lack of results for SSAH (B) and the fact that the few results are worse than the other attacks even though SSAH (B) has more information, we ignore it in what follows. All the other three attacks use the same information, there are three possible reasons for this disparity in results:

1. BIA (B) is a better algorithm for extracting information and building a potent attack from it.
2. LGV (A) and ATA (A) attacked undefended models that were somehow inherently more robust (unlikely).
3. The disparity of results is caused by the different perturbation budgets/ $l_p$ -norms used.

We suspect a combination of 1. and 3. to be the reason ex-

Model	Benign ESR (BIA)	LGV (A) ESR / Score	BIA (B) ESR / Score	ATA (A) ESR / Score	SSAH (B) ESR / Score
ResNet-50 [98]	24.39	N/A / N/A	<b>95.56</b> / <b>0.854</b>	87.31 / 0.703	N/A / N/A
VGG-16 [99]	N/A	N/A / N/A	N/A / N/A	<b>87.46</b> / N/A	19.14 / N/A
DenseNet-121 [100]	25.78	N/A / N/A	<b>96.02</b> / <b>0.856</b>	64.17 / 0.345	N/A / N/A
ResNet-152 [98]	22.66	89.6 / 0.751	<b>94.15</b> / <b>0.835</b>	N/A / N/A	N/A / N/A
VGG-19 [99]	29.05	82.2 / 0.591	<b>95.91</b> / <b>0.835</b>	N/A / N/A	N/A / N/A
Inception-v3 [101]	23.81	45.4 / 0.149	<b>85.76</b> / <b>0.679</b>	N/A / N/A	N/A / N/A
Average	25.14	72.4 / 0.497	<b>93.48</b> / <b>0.811</b>	79.65 / 0.524	19.14 / N/A
Standard deviation	2.46	23.67 / 0.312	4.38 / 0.075	13.4 / 0.253	N/A / N/A

Table 5: ImageNet dataset indistinguishable Section 6.1.1 undefended results.

plaining the discrepancy in the results. Additionally, ATA’s attack is originally meant to attack vision transformer models. Hence, it could partially explain a slightly worse performance in an equitable evaluation setting.

### 6.1.2 LGV (B) & ATA (B) & ACG

This comparison is difficult to perform, as LGV (B) and ATA (B) both attack different undefended models while not providing any benign accuracies. We can use the benign accuracy of the BIA paper as a substitute for LGV (B) but not for ATA (B). On the other hand, ACG [79] attacks only defended models, therefore we cannot directly compare with the other attacks. We compile the results in Tables 6 and 7.

Model	Benign ESR	LGV (B) ESR / Score	ATA (B) ESR / Score
ResNet-50 [98]	24.39 (BIA)	97.1 / 0.883	N/A / N/A
DeiT-T [102]	N/A	N/A / N/A	100.0 / N/A
DeiT-S [102]	N/A	N/A / N/A	100.0 / N/A
DeiT-B [102]	N/A	N/A / N/A	100.0 / N/A

Table 6: ImageNet dataset indistinguishable undefended results.

### 6.1.3 BIA (C) & SSAH (A) & Section 6.1.2

Both BIA (C) and SSAH (A) evaluate only against undefended models, therefore comparing against ACG is not possible. We can, however, compare SSAH (A) and LGV (B)

Model	Benign ESR	ACG ESR	ACG Score
ResNet-50 <sub>robustness</sub> [103]	37.44	69.58	0.344
ResNet-50 <sub>salman</sub> [104]	35.98	64.7	0.289
ResNet-18 <sub>salman</sub> [104]	47.08	74.34	0.331
WideResNet-50-2 <sub>salman</sub> [104]	31.54	60.9	0.271
ResNet-50 <sub>FAST_AT</sub> [105]	44.38	73.0	0.336
Average	39.28	68.50	0.314
Standard deviation	6.34	5.65	0.032

Table 7: ImageNet dataset indistinguishable ACG defended results.

as they both evaluate against a ResNet-50 [98]. Since SSAH (A) publishes their ResNet-50’s benign accuracy and LGV (B) does not, we also use BIA’s benign accuracy from the previous evaluation. We compute LGV (B)’s score using the mean of both benign accuracies to get closer to LGV (B)’s ResNet-50’s expected benign accuracy and get a more reliable result. BIA (C) only evaluates their white-box scenario against a VGG-16 and a DenseNet-169 in the undefended setting. We compile the results in Table 8.

Model	Benign ESR	LGV (B) ESR / Score	SSAH (A) ESR / Score	BIA (C) ESR / Score
ResNet-50 [98]	24.39 (BIA)	97.1	<b>98.56</b>	NA
	23.85 (SSAH)	0.885	<b>0.915</b>	NA
VGG-16 [99]	29.86 (BIA)	NA	NA	98.96
		NA	NA	0.890
DenseNet-169 [100]	24.25 (BIA)	NA	NA	96.68
		NA	NA	0.876
Average	26.08	97.1 0.885	<b>98.56</b> <b>0.915</b>	97.82 0.883
Standard deviation	3.28	NA	NA	1.61
		NA	NA	0.010

Table 8: ImageNet dataset indistinguishable Section 6.1.3 undefended results.

### 6.1.4 MASSA & Pixle

We include the results from MASSA [62] and Pixle [34] to complete our comparison. Since neither paper provides clean accuracies, we use the average of the benign accuracies from BIA and SSAH to compute the score. This yields the compiled results in Table 9. While MASSA evaluates its performance against defended models, they are the sole paper to use the  $l_2$ -norm for its distinguisher. Additionally, they do not provide clean accuracies for any of their models. Pixle on the other hand does not attack any defended models. Our results show

that query-based access to a model is sufficient to render it useless if the model is undefended.

Model	Benign ESR	MASSA ESR / Score	Pixle ESR / Score
ResNet-50 [98]	24.39 (BIA)	<b>99.4 / 0.930</b>	98.0 / 0.902
	23.85 (SSAH)		
VGG-16 [99]	29.86 (BIA)	<b>99.58 / 0.902</b>	99.0 / 0.891
Average	26.99	<b>99.49 / 0.916</b>	98.5 / 0.897
Standard deviation	4.06	0.12 / 0.019	0.7 / 0.008

Table 9: ImageNet dataset indistinguishable Section 6.1.4 undefended results.

## 6.2 Attacks on the CIFAR10 dataset

The second dataset we study is the CIFAR-10 dataset [96]. We can perform four comparisons on a total of seven variants of attacks. We summarize our results in Table 10.

Unsurprisingly, we find that it requires little model information to get effective attacks if the attacker has access to additional information like data and training information. Additionally, we still observe a strong transferable performance against defended models by AEG (B) where they obtain a score (0.167) very similar to white-box attacks (0.163 and 0.160). While this is still much worse than against undefended models, it would still in practice severely decrease the usability of the target model.

### 6.2.1 BIA (A) & AEG (B)

BIA (A) [8] only attack a custom model, and therefore we treat their results as unreliable. Their model achieves 6.22% benign ESR, while their attack achieves an ESR of 47.19%, yielding a score of 0.219. AEG (B) [88] on the other hand attack many common model architectures.

Model Information	Data Information	Training Information	Attack Variant	Und. ESR / Score	Def. ESR / Score
Possible Architectures	Training Data	Loss & Optimizer	AEG (B)	92.62	47.52
			BIA (A)	0.848	0.162
Architecture	Other Data	Training Function	BIA (A)	47.19	NA
			AEG (A)	0.219	NA
Scores	Same Distribution	Loss & Optimizer	AEG (A)	87.0	NA
			Pixle	NA	NA
Parameters	Same Distribution	Loss Function	SSAH (A)	100.0	NA
			A <sup>3</sup>	0.983	NA
	Same Distribution	Loss Function	A <sup>3</sup>	99.96	21.32
			ACG	0.994	0.023
Same Distribution	Loss Function	A <sup>3</sup>	NA	42.13	
		ACG	NA	0.163	
Same Distribution	Loss Function	A <sup>3</sup>	NA	41.70	
		ACG	NA	0.160	

Table 10: CIFAR-10 information and attack results. "Und." stands for undefended and "Def." stands for defended.

Since BIA (A) attacks a custom model, we have to perform an aggregate analysis of AEG (B)’s performance on both undefended and defended models to be able to compare. We report the performance on undefended / defended models in Table 11.

Model	Benign ESR	AEG (B) ESR	AEG (B) Score
VGG-16 [99]	11.2	93.8	0.867
ResNet-18 [98]	13.1	97.3	0.930
WideResNet [106]	6.8	85.2	0.721
DenseNet-121 [100]	11.2	94.1	0.873
Inception-v3 [101]	9.9	92.7	0.850
Average	10.44	92.62	0.848
Standard deviation	2.33	4.49	0.077
ResNet-18 <sub>ens3</sub> [6]	16.8	52.2	0.244
WideResNet <sub>ens3</sub> [6]	12.8	49.9	0.232
DenseNet-121 <sub>ens3</sub> [6]	21.5	41.4	0.125
Inception-v3 <sub>ens3</sub> [6]	14.8	47.5	0.204
Madry-Adv [5]	12.9	21.6	0.030
Average	15.76	47.52	0.167
Standard deviation	3.60	12.37	0.090

Table 11: CIFAR10 dataset indistinguishable AEG (B) results.

If we treat BIA (A)’s model as undefended, then AEG (B) significantly outperforms BIA (A). This could either be due to the difference in the information required by both attacks or that BIA (A) does not extract attack performance as well out of the information it uses as AEG (B).

Unsurprisingly, attacking well-defended models in the transferable setting is quite a difficult task. The results in Table 11 strongly imply that BIA (A)’s model is indeed undefended as it achieves a benign ESR much closer to the undefended models of Table 11.

### 6.2.2 A<sup>3</sup> & SSAH (A)

We can directly compare both attacks as they both attack WideResNet-34-10<sub>TRADES</sub> [107]. We can confidently confirm that these are likely to be the same models as both papers report the same benign accuracy. We present the results in Table 12.

We can see that although, as stated by the authors, A<sup>3</sup> is an attack that focuses both on ESR and runtime, it still significantly outperforms SSAH (A) when attacking a well-defended model. It is doubtful that having access to the training loss function is a strong enough difference between the

Model	Benign ESR	SSAH (A) ESR / Score	A <sup>3</sup> ESR / Score
WRN-34-10 <sub>TRADES</sub> [107]	15.08	21.32 / 0.023	<b>46.99 / 0.198</b>

Table 12: CIFAR10 dataset indistinguishable SSAH (A) and A<sup>3</sup> defended results. "WRN" stands for WideResNet.

two attacks to justify the performance gap. It is more likely that SSAH (A) is inefficient at extracting the information it has access to to mount a potent attack against defended models.

### 6.2.3 ACG & A<sup>3</sup>

We again compare ACG [79] and A<sup>3</sup> on defended models. On CIFAR10, ACG and A<sup>3</sup> attack 11 models in common from RobustBench [108]. The results are summarized in Table 13<sup>1</sup>.

Model	Benign ESR	A <sup>3</sup> ESR / Score	ACG ESR / Score
WRN-34-10 <sub>TRADES</sub> [107]	15.08	46.99 / 0.198	<b>47.18 / 0.200</b>
WRN-34-20 <sub>LBGAT</sub> [109]	11.3	<b>46.54 / 0.204</b>	46.23 / 0.201
WRN-34-10 <sub>LBGAT</sub> [109]	11.78	<b>47.24 / 0.209</b>	46.9 / 0.206
WRN-34-20 <sub>Overfitting</sub> [110]	14.66	<b>46.67 / 0.196</b>	45.69 / 0.187
WRN-70-16 <sub>Fixing</sub> [111]	11.46	<b>35.81 / 0.115</b>	35.27 / 0.111
WRN-28-10 <sub>Fixing</sub> [111]	12.67	<b>39.34 / 0.139</b>	38.8 / 0.134
WRN-28-10 <sub>AWP</sub> [112]	11.75	<b>40.02 / 0.146</b>	39.7 / 0.144
WRN-70-16 <sub>ULAT</sub> [113]	8.9	<b>34.22 / 0.109</b>	33.7 / 0.106
WRN-70-16 <sub>ULAT</sub> [113]	14.71	<b>42.92 / 0.163</b>	42.45 / 0.159
WRN-34-20 <sub>ULAT</sub> [113]	14.36	<b>43.24 / 0.166</b>	42.86 / 0.163
WRN-28-10 <sub>ULAT</sub> [113]	10.52	<b>37.3 / 0.128</b>	36.9 / 0.125
WRN-28-10 <sub>pretraining*</sub> [114]	12.89	<b>45.24 / 0.188</b>	44.75 / 0.184
Average	12.51	<b>42.13 / 0.163</b>	41.70 / 0.160
Standard deviation	1.81	4.67 / 0.036	4.72 / 0.036

Table 13: CIFAR10 dataset indistinguishable A<sup>3</sup> and ACG defended results. "WRN" stands for WideResNet.

ACG outperforms both A<sup>3</sup> and SSAH (A) on WideResNet-34-10<sub>TRADES</sub> but otherwise loses to A<sup>3</sup> on the other models and overall. We observe a small, discrepancy between ACG

<sup>1</sup>\* WideResNet-28-10<sub>pretraining</sub> misreported as WideResNet-34-10<sub>pretraining</sub> in the A<sup>3</sup> paper.



and A<sup>3</sup> in terms of performance. It could either be due to the information used or the inherent algorithmic differences. Finally, we are left with comparing all seven attacks against one another for our final comparison.

#### 6.2.4 AEG (A) & Pixle & Rest

Unfortunately, due to the amount of papers to compare, we reach the limits of what we can do while keeping the comparisons fair. We go through the few comparisons that we can still do. We first look into the straightforward comparison: AEG (A) and AEG (B). They only evaluate AEG (A) against a ResNet-18 [98]. They do not provide benign accuracies for AEG (A) which is problematic. We therefore cannot compute a relative score to attempt a comparison. We still report the ESR they report in our overall Table 10, however, we italicize the result to indicate that it is unreliable.

Our other option would be to compare AEG (B) with Pixle, as AEG (B) provides benign accuracies, and they share a target model architecture (ResNet-18). Unfortunately, Pixle does not share its benign accuracy, so we deem their results unreliable for comparison.

We get the following results in Table 14.

Model	Benign ESR	AEG (B) ESR / Score	Pixle ESR / Score
ResNet-18 [98]	13.1	97.3 / 0.930	<i>100.0 / 0.983</i>

Table 14: CIFAR10 dataset indistinguishable AEG (B) & Pixle undefended results.

## 7 Takeaways

1. **Undefended models are broken.** This is not a particularly new finding, but we confirm and reinforce it. We show that across all datasets and threat models studied, not once are undefended models robust to attacks. On CIFAR-10, the undefended worst and best scores are, respectively, 0.219, and 0.994. Whereas, the defended worst and best scores are, respectively, 0.023, and 0.163. Even the best attack on defended models does not perform as well as the worst attack on undefended models.
2. **The transferable setting might not be as difficult as previously thought.** We noticed that transferable attacks, when given additional information like access to the training data and training information such as the training function, can perform very well, almost on par with white-box attacks. For CIFAR-10, the best transferable attack is only within 7.3% ESR / 0.146 score of the best white-box attack. This reinforces the notion that any information given to the attacker is crucial.
3. **Information categories matter, but their effect on performance is not straightforward.** Information’s effect

on performance is highly dependent on the other information available. For example, in the white-box setting, data and training information are nominal. But in the transferable setting, they are crucial. In particular, training data information seems to be critical to attack performance. This is best observed when looking at BIA (A) on the CIFAR-10 dataset. They severely underperform other transferable attacks (47.2% ESR / 0.22 score compared to 87.0% ESR and 92.6% ESR / 0.85 score for its closest competitors AEG(A) & (B)). Not having access to the training data or even data from the same distribution appears to severely affect attack performance.

4. **Training information is understated but essential to transferable attacks.** Most of the transferable attacks whose results we have studied use the training function. This is done to train surrogate models. However, this assumption is not explicitly stated in the papers we survey and is instead taken for granted. It goes against proper security practices as it omits what our results clearly show to be critical information in the threat model description.
5. **Need for better standard evaluation frameworks.** There is a surprising lack of standards to evaluate adversarial example attacks. This unnecessarily complicates comparisons between existing works that are not directly related. Only two papers (ACG and A<sup>3</sup>) used an existing evaluation framework (Robustbench [108]).
6. **Evaluation against defended models.** Too few papers evaluate their attack against defended models (and they usually evaluate too few defended models as well when they do). Only one paper evaluates its attack against defended models on ImageNet and only four papers do so on CIFAR-10. Papers that only evaluate undefended models bring little to the field as a whole as we have seen it is not a meaningful measure of attack quality.

## 8 Conclusion

In this work, we presented a formalization to study adversary knowledge in the context of adversarial example attacks on image classification models. We were able to systematize a large body of existing work into our framework and are confident in its ability to extend to future research in adversarial example attacks and defenses. Our work can be used to enhance the reproducibility, comparability and fairness of such future work as it allows a precise description of one’s threat model and evaluations.

## Acknowledgments

We gratefully acknowledge the support of the Natural Sciences and Engineering Research Council (NSERC) for grants RGPIN-2023-03244, and IRC-537591 and the Royal Bank of Canada.

## References

- [1] Hafsa Habehh1 and Suril Gohel. Machine learning in healthcare. *national library of medicine*, 2021. doi: 10.2174/1389202922666210705124359.
- [2] Abhishek Gupta, Alagan Anpalagan, Ling Guan, and Ahmed Shaharyar Khwaja. Deep learning for object detection and scene perception in self-driving cars: Survey, challenges, and open issues. *Array*, 10:100057, 2021. ISSN 2590-0056. doi: <https://doi.org/10.1016/j.array.2021.100057>. URL <https://www.sciencedirect.com/science/article/pii/S2590005621000059>.
- [3] Zhehan Ni. Reframe the field of aerospace engineering via machine learning: Application and comparison. *Journal of Physics: Conference Series*, 2386(1):012031, dec 2022. doi: 10.1088/1742-6596/2386/1/012031. URL <https://dx.doi.org/10.1088/1742-6596/2386/1/012031>.
- [4] Christian Szegedy, Wojciech Zaremba, Ilya Sutskever, Joan Bruna, Dumitru Erhan, Ian Goodfellow, and Rob Fergus. Intriguing properties of neural networks, 2014.
- [5] Aleksander Madry, Aleksandar Makelov, Ludwig Schmidt, Dimitris Tsipras, and Adrian Vladu. Towards deep learning models resistant to adversarial attacks, 2019.
- [6] Florian Tramèr, Alexey Kurakin, Nicolas Papernot, Ian Goodfellow, Dan Boneh, and Patrick McDaniel. Ensemble adversarial training: Attacks and defenses, 2020.
- [7] Jeremy Cohen, Elan Rosenfeld, and Zico Kolter. Certified adversarial robustness via randomized smoothing. In *international conference on machine learning*, pages 1310–1320. PMLR, 2019.
- [8] Qilong Zhang, Xiaodan Li, Yuefeng Chen, Jingkuan Song, Lianli Gao, Yuan He, and Hui Xue. Beyond imagenet attack: Towards crafting adversarial examples for black-box domains, 2022.
- [9] Jiyuan Liu, Bingyi Lu, Mingkang Xiong, Tao Zhang, and Huilin Xiong. Adversarial attack with raindrops. (arXiv:2302.14267), July 2023. doi: 10.48550/arXiv.2302.14267. URL <http://arxiv.org/abs/2302.14267>. arXiv:2302.14267 [cs].
- [10] Fahad Shamshad, Muzammal Naseer, and Karthik Nandakumar. Clip2protect: Protecting facial privacy using text-guided makeup via adversarial latent search. page 20595–20605, 2023. URL [https://openaccess.thecvf.com/content/CVPR2023/html/Shamshad\\_CLIP2Protect\\_Protecting\\_Facial\\_Privacy\\_Using\\_Text-Guided\\_Makeup\\_via\\_Adversarial\\_Latent\\_CVPR\\_2023\\_paper.html](https://openaccess.thecvf.com/content/CVPR2023/html/Shamshad_CLIP2Protect_Protecting_Facial_Privacy_Using_Text-Guided_Makeup_via_Adversarial_Latent_CVPR_2023_paper.html).
- [11] Yiqi Zhong, Xianming Liu, Deming Zhai, Junjun Jiang, and Xiangyang Ji. Shadows can be dangerous: Stealthy and effective physical-world adversarial attack by natural phenomenon. In *Proceedings of the IEEE/CVF Conference on Computer Vision and Pattern Recognition (CVPR)*, pages 15345–15354, June 2022.
- [12] Junhua Zou, Yexin Duan, Boyu Li, Wu Zhang, Yu Pan, and Zhisong Pan. Making adversarial examples more transferable and indistinguishable. *Proceedings of the AAAI Conference on Artificial Intelligence*, 36(33):3662–3670, June 2022. ISSN 2374-3468. doi: 10.1609/aaai.v36i3.20279.
- [13] Xingxing Wei and Shiji Zhao. Boosting adversarial transferability with learnable patch-wise masks. *IEEE Transactions on Multimedia*, page 1–10, 2023. ISSN 1941-0077. doi: 10.1109/TMM.2023.3315550.
- [14] Zhipeng Wei, Jingjing Chen, Zuxuan Wu, and Yu-Gang Jiang. Enhancing the self-universality for transferable targeted attacks. page 12281–12290, 2023. URL [https://openaccess.thecvf.com/content/CVPR2023/html/Wei\\_Enhancing\\_the\\_Self-Universality\\_for\\_Transferable\\_Targeted\\_Attacks\\_CVPR\\_2023\\_paper.html](https://openaccess.thecvf.com/content/CVPR2023/html/Wei_Enhancing_the_Self-Universality_for_Transferable_Targeted_Attacks_CVPR_2023_paper.html).
- [15] Juanjuan Weng, Zhiming Luo, Dazhen Lin, Shaozi Li, and Zhun Zhong. Boosting adversarial transferability via fusing logits of top-1 decomposed feature. (arXiv:2305.01361), July 2023. doi: 10.48550/arXiv.2305.01361. URL <http://arxiv.org/abs/2305.01361>. arXiv:2305.01361 [cs].
- [16] Yaoyuan Zhang, Yu-an Tan, Haipeng Sun, Yuhang Zhao, Quanxing Zhang, and Yuanzhang Li. Improving the invisibility of adversarial examples with perceptually adaptive perturbation. *Information Sciences*, 635:126–137, July 2023. ISSN 0020-0255. doi: 10.1016/j.ins.2023.03.139.
- [17] Donald C. Wunsch Tao Wu, Tie Luo. Black-box attack using adversarial examples: A new method of improving transferability. URL <https://www.worldscientific.com/doi/10.1142/S2811032322500059>.
- [18] Juanjuan Weng, Zhiming Luo, Shaozi Li, Nicu Sebe, and Zhun Zhong. Logit margin matters: Improving transferable targeted adversarial attack by logit calibration. *IEEE Transactions on Information Forensics and Security*, 18:3561–3574, 2023. doi: 10.1109/TIFS.2023.3284649.

- [19] Zhengjie Deng, Wen Xiao, Xiyan Li, Shuqian He, and Yizhen Wang. Enhancing the transferability of targeted attacks with adversarial perturbation transform. *Electronics*, 12(1818):3895, January 2023. ISSN 2079-9292. doi: 10.3390/electronics12183895.
- [20] Zhijin Ge, Fanhua Shang, Hongying Liu, Yuanyuan Liu, and Xiaosen Wang. Boosting adversarial transferability by achieving flat local maxima. (arXiv:2306.05225), June 2023. doi: 10.48550/arXiv.2306.05225. URL <http://arxiv.org/abs/2306.05225>. arXiv:2306.05225 [cs].
- [21] Zhijin Ge, Fanhua Shang, Hongying Liu, Yuanyuan Liu, Liang Wan, Wei Feng, and Xiaosen Wang. Improving the transferability of adversarial examples with arbitrary style transfer. August 2023. doi: 10.1145/3581783.3612070. URL <http://arxiv.org/abs/2308.10601>. arXiv:2308.10601 [cs, eess].
- [22] Hongying Liu, Zhijin Ge, Zhenyu Zhou, Fanhua Shang, Yuanyuan Liu, and Licheng Jiao. Gradient correction for white-box adversarial attacks. *IEEE Transactions on Neural Networks and Learning Systems*, page 1–12, 2023. ISSN 2162-2388. doi: 10.1109/TNNLS.2023.3315414.
- [23] Zhibo Wang, Hongshan Yang, Yunhe Feng, Peng Sun, Hengchang Guo, Zhifei Zhang, and Kui Ren. Towards transferable targeted adversarial examples. page 20534–20543, 2023. URL [https://openaccess.thecvf.com/content/CVPR2023/html/Wang\\_Towards\\_Transferable\\_Targeted\\_Adversarial\\_Examples\\_CVPR\\_2023\\_paper.html](https://openaccess.thecvf.com/content/CVPR2023/html/Wang_Towards_Transferable_Targeted_Adversarial_Examples_CVPR_2023_paper.html).
- [24] Florian Tramer. Detecting adversarial examples is (nearly) as hard as classifying them. In *Proceedings of the 39th International Conference on Machine Learning*, page 21692–21702. PMLR, June 2022. URL <https://proceedings.mlr.press/v162/tramer22a.html>.
- [25] Junyoung Byun, Myung-Joon Kwon, Seungju Cho, Yoonji Kim, and Changick Kim. Introducing competition to boost the transferability of targeted adversarial examples through clean feature mixup. page 24648–24657, 2023. URL [https://openaccess.thecvf.com/content/CVPR2023/html/Byun\\_Introducing\\_Competition\\_To\\_Boost\\_the\\_Transferability\\_of\\_Targeted\\_Adversarial\\_Examples\\_CVPR\\_2023\\_paper.html](https://openaccess.thecvf.com/content/CVPR2023/html/Byun_Introducing_Competition_To_Boost_the_Transferability_of_Targeted_Adversarial_Examples_CVPR_2023_paper.html).
- [26] Bin Chen, Jiali Yin, Shukai Chen, Bohao Chen, and Ximeng Liu. An adaptive model ensemble adversarial attack for boosting adversarial transferability. page 4489–4498, 2023. URL [https://openaccess.thecvf.com/content/ICCV2023/html/Chen\\_An\\_Adaptive\\_Model\\_Ensemble\\_Adversarial\\_Attack\\_for\\_Boosting\\_Adversarial\\_Transferability\\_ICCV\\_2023\\_paper.html](https://openaccess.thecvf.com/content/ICCV2023/html/Chen_An_Adaptive_Model_Ensemble_Adversarial_Attack_for_Boosting_Adversarial_Transferability_ICCV_2023_paper.html).
- [27] Qizhang Li, Yiwen Guo, Xiaochen Yang, Wangmeng Zuo, and Hao Chen. Improving transferability of adversarial examples via bayesian attacks. (arXiv:2307.11334), July 2023. doi: 10.48550/arXiv.2307.11334. URL <http://arxiv.org/abs/2307.11334>. arXiv:2307.11334 [cs].
- [28] Qizhang Li, Yiwen Guo, Wangmeng Zuo, and Hao Chen. Making substitute models more bayesian can enhance transferability of adversarial examples. (arXiv:2302.05086), July 2023. doi: 10.48550/arXiv.2302.05086. URL <http://arxiv.org/abs/2302.05086>. arXiv:2302.05086 [cs].
- [29] Zeyu Qin, Yanbo Fan, Yi Liu, Li Shen, Yong Zhang, Jue Wang, and Baoyuan Wu. Boosting the transferability of adversarial attacks with reverse adversarial perturbation. *Advances in Neural Information Processing Systems*, 35:29845–29858, December 2022.
- [30] Xiangyuan Yang, Jie Lin, Hanlin Zhang, Xinyu Yang, and Peng Zhao. Improving the transferability of adversarial examples via direction tuning. (arXiv:2303.15109), August 2023. doi: 10.48550/arXiv.2303.15109. URL <http://arxiv.org/abs/2303.15109>. arXiv:2303.15109 [cs].
- [31] Yulong Yang, Chenhao Lin, Qian Li, Chao Shen, Dawei Zhou, Nannan Wang, and Tongliang Liu. Quantization aware attack: Enhancing the transferability of adversarial attacks across target models with different quantization bitwidths. (arXiv:2305.05875), May 2023. doi: 10.48550/arXiv.2305.05875. URL <http://arxiv.org/abs/2305.05875>. arXiv:2305.05875 [cs].
- [32] Xiangyu Qi, Kaixuan Huang, Ashwinee Panda, Peter Henderson, Mengdi Wang, and Prateek Mittal. Visual adversarial examples jailbreak aligned large language models. (arXiv:2306.13213), August 2023. doi: 10.48550/arXiv.2306.13213. URL <http://arxiv.org/abs/2306.13213>. arXiv:2306.13213 [cs].
- [33] Maura Pintor, Luca Demetrio, Angelo Sotgiu, Ambra Demontis, Nicholas Carlini, Battista Biggio, and Fabio Roli. Indicators of attack failure: Debugging and improving optimization of adversarial examples. *Advances in Neural Information Processing Systems*, 35:23063–23076, December 2022.
- [34] Jary Pomponi, Simone Scardapane, and Aurelio Uncini. Pixle: a fast and effective black-box attack based on

- rearranging pixels. In *2022 International Joint Conference on Neural Networks (IJCNN)*. IEEE, jul 2022. doi: 10.1109/ijcnn55064.2022.9892966. URL <https://doi.org/10.1109%2Fijcnn55064.2022.9892966>.
- [35] Xiu-Chuan Li, Xu-Yao Zhang, Fei Yin, and Cheng-Lin Liu. Decision-based adversarial attack with frequency mixup. *IEEE Transactions on Information Forensics and Security*, 17:1038–1052, 2022. doi: 10.1109/TIFS.2022.3156809.
- [36] Ye Liu, Yaya Cheng, Lianli Gao, Xianglong Liu, Qilong Zhang, and Jingkuan Song. Practical evaluation of adversarial robustness via adaptive auto attack. In *Proceedings of the IEEE/CVF Conference on Computer Vision and Pattern Recognition*, pages 15105–15114, 2022.
- [37] Fangcheng Liu, Chao Zhang, and Hongyang Zhang. Towards transferable unrestricted adversarial examples with minimum changes, 2022.
- [38] Giovanni Apruzzese, Hyrum S. Anderson, Savino Dambra, David Freeman, Fabio Pierazzi, and Kevin Roundy. “real attackers don’t compute gradients”: Bridging the gap between adversarial ml research and practice. In *2023 IEEE Conference on Secure and Trustworthy Machine Learning (SaTML)*, page 339–364, February 2023. doi: 10.1109/SaTML54575.2023.00031.
- [39] Akshay Agarwal, Nalini Ratha, Mayank Vatsa, and Richa Singh. Exploring robustness connection between artificial and natural adversarial examples. page 179–186, 2022. URL [https://openaccess.thecvf.com/content/CVPR2022W/ArtOfRobust/html/Agarwal\\_Exploring\\_Robustness\\_Connection\\_Between\\_Artificial\\_and\\_Natural\\_Adversarial\\_Examples\\_CVPRW\\_2022\\_paper.html](https://openaccess.thecvf.com/content/CVPR2022W/ArtOfRobust/html/Agarwal_Exploring_Robustness_Connection_Between_Artificial_and_Natural_Adversarial_Examples_CVPRW_2022_paper.html).
- [40] Ahmed Aldahdooh, Wassim Hamidouche, Sid Ahmed Fezza, and Olivier Déforges. Adversarial example detection for dnn models: a review and experimental comparison. *Artificial Intelligence Review*, 55(6): 4403–4462, August 2022. ISSN 1573-7462. doi: 10.1007/s10462-021-10125-w.
- [41] Enes Altinisik, Safa Messaoud, Husrev Taha Sencar, and Sanjay Chawla. A3t: accuracy aware adversarial training. *Machine Learning*, 112(9):3191–3210, September 2023. ISSN 1573-0565. doi: 10.1007/s10994-023-06341-w.
- [42] Junyoung Byun, Seungju Cho, Myung-Joon Kwon, Hee-Seon Kim, and Changick Kim. Improving the transferability of targeted adversarial examples through object-based diverse input. In *Proceedings of the IEEE/CVF Conference on Computer Vision and Pattern Recognition (CVPR)*, pages 15244–15253, June 2022.
- [43] Bin Chen, Yan Feng, Tao Dai, Jiawang Bai, Yong Jiang, Shu-Tao Xia, and Xuan Wang. Adversarial examples generation for deep product quantization networks on image retrieval. *IEEE Transactions on Pattern Analysis and Machine Intelligence*, 45(2):1388–1404, 2023. doi: 10.1109/TPAMI.2022.3165024.
- [44] Pin-Yu Chen and Sijia Liu. Holistic adversarial robustness of deep learning models. *Proceedings of the AAAI Conference on Artificial Intelligence*, 37(1313): 15411–15420, September 2023. ISSN 2374-3468. doi: 10.1609/aaai.v37i13.26797.
- [45] Francesco Crecchi, Marco Melis, Angelo Sotgiu, Davide Bacciu, and Battista Biggio. Fader: Fast adversarial example rejection. *Neurocomputing*, 470: 257–268, January 2022. ISSN 0925-2312. doi: 10.1016/j.neucom.2021.10.082.
- [46] Tao Dai, Yan Feng, Bin Chen, Jian Lu, and Shu-Tao Xia. Deep image prior based defense against adversarial examples. *Pattern Recognition*, 122:108249, February 2022. ISSN 0031-3203. doi: 10.1016/j.patcog.2021.108249.
- [47] Aeryn Dunmore, Julian Jang-Jaccard, Fariza Sabrina, and Jin Kwak. A comprehensive survey of generative adversarial networks (gans) in cybersecurity intrusion detection. *IEEE Access*, 11:76071–76094, 2023. ISSN 2169-3536. doi: 10.1109/ACCESS.2023.3296707.
- [48] Salijona Dyrmishi, Salah Ghamizi, Thibault Simonetto, Yves Le Traon, and Maxime Cordy. On the empirical effectiveness of unrealistic adversarial hardening against realistic adversarial attacks. In *2023 IEEE Symposium on Security and Privacy (SP)*, page 1384–1400, May 2023. doi: 10.1109/SP46215.2023.10179316.
- [49] Timo Freiesleben. The intriguing relation between counterfactual explanations and adversarial examples. *Minds and Machines*, 32(1):77–109, March 2022. ISSN 1572-8641. doi: 10.1007/s11023-021-09580-9.
- [50] Weiyuan Gong and Dong-Ling Deng. Universal adversarial examples and perturbations for quantum classifiers. *National Science Review*, 9(6):nwab130, June 2022. ISSN 2095-5138. doi: 10.1093/nsr/nwab130.
- [51] Martin Gubri, Maxime Cordy, Mike Papadakis, Yves Le Traon, and Koushik Sen. Lgv: Boosting adversarial example transferability from large geometric vicinity. In Shai Avidan, Gabriel Brostow, Moustapha



- Cissé, Giovanni Maria Farinella, and Tal Hassner, editors, *Computer Vision – ECCV 2022*, page 603–618, Cham, 2022. Springer Nature Switzerland. ISBN 978-3-031-19772-7.
- [52] Carlos Javier Hernández-Castro, Zhuoran Liu, Alex Serban, Ilias Tsingenopoulos, and Wouter Joosen. *Adversarial Machine Learning*, page 287–312. Lecture Notes in Computer Science. Springer International Publishing, Cham, 2022. ISBN 978-3-030-98795-4. doi: 10.1007/978-3-030-98795-4\_12. URL [https://doi.org/10.1007/978-3-030-98795-4\\_12](https://doi.org/10.1007/978-3-030-98795-4_12).
- [53] Zichao Hu, Heng Li, Liheng Yuan, Zhang Cheng, Wei Yuan, and Ming Zhu. Model scheduling and sample selection for ensemble adversarial example attacks. *Pattern Recognition*, 130:108824, October 2022. ISSN 0031-3203. doi: 10.1016/j.patcog.2022.108824.
- [54] Z. O. U. Jun-hua, Duan Ye-xin, R. E. N. Chuan-lun, Q. I. U. Jun-yang, Zhou Xing-yu, and P. a. N. Zhi-song. Perturbation initialization, adam-nesterov and quasi-hyperbolic momentum for adversarial examples. *ACTA ELECTRONICA SINICA*, 50(1):207, January 2022. ISSN 0372-2112. doi: 10.12263/DZXB.20200839.
- [55] Minjong Lee and Dongwoo Kim. Robust evaluation of diffusion-based adversarial purification. (arXiv:2303.09051), August 2023. doi: 10.48550/arXiv.2303.09051. URL <http://arxiv.org/abs/2303.09051>. arXiv:2303.09051 [cs].
- [56] Yao Li, Minhao Cheng, Cho-Jui Hsieh, and Thomas C. M. Lee. A review of adversarial attack and defense for classification methods. *The American Statistician*, 76(4):329–345, October 2022. ISSN 0003-1305. doi: 10.1080/00031305.2021.2006781.
- [57] Chumeng Liang, Xiaoyu Wu, Yang Hua, Jiaru Zhang, Yiming Xue, Tao Song, Zhengui Xue, Ruhui Ma, and Haibing Guan. Adversarial example does good: Preventing painting imitation from diffusion models via adversarial examples. June 2023. URL <https://openreview.net/forum?id=Wbquvk97t4>.
- [58] Hongshuo Liang, Erlu He, Yangyang Zhao, Zhe Jia, and Hao Li. Adversarial attack and defense: A survey. *Electronics*, 11(88):1283, January 2022. ISSN 2079-9292. doi: 10.3390/electronics11081283.
- [59] Chang-Sheng Lin, Chia-Yi Hsu, Pin-Yu Chen, and Chia-Mu Yu. Real-world adversarial examples via makeup. In *ICASSP 2022 - 2022 IEEE International Conference on Acoustics, Speech and Signal Processing (ICASSP)*, page 2854–2858, May 2022. doi: 10.1109/ICASSP43922.2022.9747469.
- [60] Jiabao Liu, Qixiang Zhang, Kanghua Mo, Xiaoyu Xiang, Jin Li, Debin Cheng, Rui Gao, Beishui Liu, Kongyang Chen, and Guanjie Wei. An efficient adversarial example generation algorithm based on an accelerated gradient iterative fast gradient. *Computer Standards & Interfaces*, 82:103612, August 2022. ISSN 0920-5489. doi: 10.1016/j.csi.2021.103612.
- [61] Cheng Luo, Qinliang Lin, Weicheng Xie, Bizhu Wu, Jinheng Xie, and Linlin Shen. Frequency-driven imperceptible adversarial attack on semantic similarity. In *Proceedings of the IEEE/CVF Conference on Computer Vision and Pattern Recognition (CVPR)*, pages 15315–15324, June 2022.
- [62] Kim A. B. Midtliid, Johannes Åsheim, and Jingyue Li. Magnitude adversarial spectrum search-based black-box attack against image classification. In *Proceedings of the 15th ACM Workshop on Artificial Intelligence and Security, AISec’22*, page 67–77, New York, NY, USA, 2022. Association for Computing Machinery. ISBN 9781450398800. doi: 10.1145/3560830.3563723. URL <https://doi.org/10.1145/3560830.3563723>.
- [63] Dmitry Namiot and Eugene Ilyushin. Generative models in machine learning. *International Journal of Open Information Technologies*, 10(77):101–118, June 2022. ISSN 2307-8162.
- [64] Tianyu Pang, Huishuai Zhang, Di He, Yinpeng Dong, Hang Su, Wei Chen, Jun Zhu, and Tie-Yan Liu. Two coupled rejection metrics can tell adversarial examples apart. page 15223–15233, 2022. URL [https://openaccess.thecvf.com/content/CVPR2022/html/Pang\\_Two\\_Coupled\\_Rejection\\_Metrics\\_Can\\_Tell\\_Adversarial\\_Examples\\_Apart\\_CVPR\\_2022\\_paper.html](https://openaccess.thecvf.com/content/CVPR2022/html/Pang_Two_Coupled_Rejection_Metrics_Can_Tell_Adversarial_Examples_Apart_CVPR_2022_paper.html).
- [65] Martin Pawelczyk, Chirag Agarwal, Shalmali Joshi, Sohini Upadhyay, and Himabindu Lakkaraju. Exploring counterfactual explanations through the lens of adversarial examples: A theoretical and empirical analysis. In *Proceedings of The 25th International Conference on Artificial Intelligence and Statistics*, page 4574–4594. PMLR, May 2022. URL <https://proceedings.mlr.press/v151/pawelczyk22a.html>.
- [66] Rafael Pinot, Laurent Meunier, Florian Yger, Cédric Gouy-Pailler, Yann Chevaleyre, and Jamal Atif. On the robustness of randomized classifiers to adversarial examples. *Machine Learning*, 111(9):3425–3457, September 2022. ISSN 1573-0565. doi: 10.1007/s10994-022-06216-6.

- [67] Peihan Qi, Tao Jiang, Lizhan Wang, Xu Yuan, and Zan Li. Detection tolerant black-box adversarial attack against automatic modulation classification with deep learning. *IEEE Transactions on Reliability*, 71(2):674–686, 2022. doi: 10.1109/TR.2022.3161138.
- [68] Zhuang Qian, Kaizhu Huang, Qiu-Feng Wang, and Xu-Yao Zhang. A survey of robust adversarial training in pattern recognition: Fundamental, theory, and methodologies. *Pattern Recognition*, 131:108889, November 2022. ISSN 0031-3203. doi: 10.1016/j.patcog.2022.108889.
- [69] Nataniel Ruiz, Adam Kortylewski, Weichao Qiu, Cihang Xie, Sarah Adel Bargal, Alan Yuille, and Stan Sclaroff. Simulated adversarial testing of face recognition models. page 4145–4155, 2022. URL [https://openaccess.thecvf.com/content/CVPR2022/html/Ruiz\\_Simulated\\_Adversarial\\_Testing\\_of\\_Face\\_Recognition\\_Models\\_CVPR\\_2022\\_paper.html](https://openaccess.thecvf.com/content/CVPR2022/html/Ruiz_Simulated_Adversarial_Testing_of_Face_Recognition_Models_CVPR_2022_paper.html).
- [70] Afia Sajeeda and B M Mainul Hossain. Exploring generative adversarial networks and adversarial training. *International Journal of Cognitive Computing in Engineering*, 3:78–89, June 2022. ISSN 26663074. doi: 10.1016/j.ijcce.2022.03.002.
- [71] Amitoj Bir Singh, Lalit Kumar Awasthi, and Urvashi. Defense against adversarial attacks using chained dual-gan approach. In R. Asokan, Diego P. Ruiz, Zubair A. Baig, and Selwyn Piramuthu, editors, *Smart Data Intelligence*, Algorithms for Intelligent Systems, page 121–133, Singapore, 2022. Springer Nature. ISBN 978-981-19331-1-0. doi: 10.1007/978-981-19-3311-0\_11.
- [72] Omer Faruk Tuna, Ferhat Ozgur Catak, and M. Taner Eskil. Closeness and uncertainty aware adversarial examples detection in adversarial machine learning. *Computers and Electrical Engineering*, 101:107986, July 2022. ISSN 0045-7906. doi: 10.1016/j.compeleceng.2022.107986.
- [73] Daniël Vos and Sicco Verwer. Robust optimal classification trees against adversarial examples. *Proceedings of the AAAI Conference on Artificial Intelligence*, 36(88):8520–8528, June 2022. ISSN 2374-3468. doi: 10.1609/aaai.v36i8.20829.
- [74] Ryan Sheatsley, Blaine Hoak, Eric Pauley, and Patrick McDaniel. The space of adversarial strategies. (arXiv:2209.04521), September 2022. doi: 10.48550/arXiv.2209.04521. URL <http://arxiv.org/abs/2209.04521>. arXiv:2209.04521 [cs].
- [75] Martin Gubri, Maxime Cordy, and Yves Le Traon. Going further: Flatness at the rescue of early stopping for adversarial example transferability. (arXiv:2304.02688), April 2023. doi: 10.48550/arXiv.2304.02688. URL <http://arxiv.org/abs/2304.02688>. arXiv:2304.02688 [cs, stat].
- [76] Huanhuan Li, Wenbo Yu, and He Huang. Strengthening transferability of adversarial examples by adaptive inertia and amplitude spectrum dropout. *Neural Networks*, 165:925–937, August 2023. ISSN 0893-6080. doi: 10.1016/j.neunet.2023.06.031.
- [77] Yan Fang, Zhongyuan Wang, Jikang Cheng, Ruoxi Wang, and Chao Liang. Promoting adversarial transferability with enhanced loss flatness. In *2023 IEEE International Conference on Multimedia and Expo (ICME)*, pages 1217–1222, 2023. doi: 10.1109/ICME55011.2023.00212.
- [78] Yuxuan Wang, Jiakai Wang, Zixin Yin, Ruihao Gong, Jingyi Wang, Aishan Liu, and Xianglong Liu. Generating transferable adversarial examples against vision transformers. In *Proceedings of the 30th ACM International Conference on Multimedia*, MM ’22, page 5181–5190, New York, NY, USA, 2022. Association for Computing Machinery. ISBN 9781450392037. doi: 10.1145/3503161.3547989. URL <https://doi.org/10.1145/3503161.3547989>.
- [79] Keiichiro Yamamura, Haruki Sato, Nariaki Tateiwa, Nozomi Hata, Toru Mitsutake, Issa Oe, Hiroki Ishikura, and Katsuki Fujisawa. Diversified adversarial attacks based on conjugate gradient method. In Kamalika Chaudhuri, Stefanie Jegelka, Le Song, Csaba Szepesvari, Gang Niu, and Sivan Sabato, editors, *Proceedings of the 39th International Conference on Machine Learning*, volume 162 of *Proceedings of Machine Learning Research*, pages 24872–24894. PMLR, 17–23 Jul 2022. URL <https://proceedings.mlr.press/v162/yamamura22a.html>.
- [80] Yuyang Long, Qilong Zhang, Boheng Zeng, Lianli Gao, Xianglong Liu, Jian Zhang, and Jingkuan Song. Frequency domain model augmentation for adversarial attack. In *European Conference on Computer Vision*, pages 549–566. Springer, 2022.
- [81] Zhaoyu Chen, Bo Li, Shuang Wu, Jianghe Xu, Shouhong Ding, and Wenqiang Zhang. Shape matters: deformable patch attack. In *European conference on computer vision*, pages 529–548. Springer, 2022.
- [82] Jianqi Chen, Hao Chen, Keyan Chen, Yilan Zhang, Zhengxia Zou, and Zhenwei Shi. Diffusion models for imperceptible and transferable adversarial attack, 2023.
- [83] Zhaoyu Chen, Bo Li, Shuang Wu, Kaixun Jiang, Shouhong Ding, and Wenqiang Zhang. Content-based unrestricted adversarial attack, 2023.

- [84] Xuelong Dai, Kaisheng Liang, and Bin Xiao. Advdiff: Generating unrestricted adversarial examples using diffusion models, 2023.
- [85] Jiang Liu, Chun Pong Lau, and Rama Chellappa. Diffprotect: Generate adversarial examples with diffusion models for facial privacy protection, 2023.
- [86] Shuo-Yen Lin, Ernie Chu, Che-Hsien Lin, Jun-Cheng Chen, and Jia-Ching Wang. Diffusion to confusion: Naturalistic adversarial patch generation based on diffusion model for object detector, 2023.
- [87] Weili Nie, Brandon Guo, Yujia Huang, Chaowei Xiao, Arash Vahdat, and Anima Anandkumar. Diffusion models for adversarial purification. *arXiv preprint arXiv:2205.07460*, 2022.
- [88] Joey Bose, Gauthier Gidel, Hugo Berard, Andre Cianflone, Pascal Vincent, Simon Lacoste-Julien, and Will Hamilton. Adversarial example games. *Advances in neural information processing systems*, 33:8921–8934, 2020.
- [89] Xiaosen Wang, Xuanran He, Jingdong Wang, and Kun He. Admix: Enhancing the transferability of adversarial attacks. In *Proceedings of the IEEE/CVF International Conference on Computer Vision (ICCV)*, pages 16158–16167, October 2021.
- [90] Tao Bai, Jun Zhao, Jinlin Zhu, Shoudong Han, Jiefeng Chen, Bo Li, and Alex Kot. Ai-gan: Attack-inspired generation of adversarial examples. In *2021 IEEE International Conference on Image Processing (ICIP)*, pages 2543–2547, 2021. doi: 10.1109/ICIP42928.2021.9506278.
- [91] Nicolas Papernot, Patrick McDaniel, Arunesh Sinha, and Michael P. Wellman. Sok: Security and privacy in machine learning. In *2018 IEEE European Symposium on Security and Privacy (EuroSP)*, pages 399–414, 2018. doi: 10.1109/EuroSP.2018.00035.
- [92] Nicholas Carlini and David Wagner. Towards evaluating the robustness of neural networks. In *2017 IEEE Symposium on Security and Privacy (SP)*, pages 39–57, 2017. doi: 10.1109/SP.2017.49.
- [93] Yuefeng Chen, Xiaofeng Mao, Yuan He, Hui Xue, Chao Li, Yinpeng Dong, Qi-An Fu, Xiao Yang, Wenzhao Xiang, Tianyu Pang, Hang Su, Jun Zhu, Fangcheng Liu, Chao Zhang, Hongyang Zhang, Yichi Zhang, Shilong Liu, Chang Liu, Wenzhao Xiang, Yajie Wang, Huipeng Zhou, Haoran Lyu, Yidan Xu, Zixuan Xu, Taoyu Zhu, Wenjun Li, Xianfeng Gao, Guoqiu Wang, Huanqian Yan, Ying Guo, Chaoning Zhang, Zheng Fang, Yang Wang, Bingyang Fu, Yunfei Zheng, Yekui Wang, Haorong Luo, and Zhen Yang. Unrestricted adversarial attacks on imagenet competition, 2021.
- [94] Justin Gilmer, Ryan P. Adams, Ian Goodfellow, David Andersen, and George E. Dahl. Motivating the rules of the game for adversarial example research, 2018.
- [95] Yann LeCun. The mnist database of handwritten digits, 1998. In *Technical report*.
- [96] Alex Krizhevsky. Learning multiple layers of features from tiny images, 2009. In *Technical report*.
- [97] Jia Deng, Wei Dong, Richard Socher, Li-Jia Li, Kai Li, and Li Fei-Fei. Imagenet: A large-scale hierarchical image database. In *2009 IEEE conference on computer vision and pattern recognition*, pages 248–255. Ieee, 2009.
- [98] Kaiming He, Xiangyu Zhang, Shaoqing Ren, and Jian Sun. Deep residual learning for image recognition. In *Proceedings of the IEEE Conference on Computer Vision and Pattern Recognition (CVPR)*, June 2016.
- [99] Karen Simonyan and Andrew Zisserman. Very deep convolutional networks for large-scale image recognition, 2015.
- [100] Gao Huang, Zhuang Liu, Laurens van der Maaten, and Kilian Q. Weinberger. Densely connected convolutional networks. In *Proceedings of the IEEE Conference on Computer Vision and Pattern Recognition (CVPR)*, July 2017.
- [101] Christian Szegedy, Vincent Vanhoucke, Sergey Ioffe, Jon Shlens, and Zbigniew Wojna. Rethinking the inception architecture for computer vision. In *Proceedings of the IEEE Conference on Computer Vision and Pattern Recognition (CVPR)*, June 2016.
- [102] Hugo Touvron, Matthieu Cord, Matthijs Douze, Francisco Massa, Alexandre Sablayrolles, and Hervé Jégou. Training data-efficient image transformers & distillation through attention. In *International conference on machine learning*, pages 10347–10357. PMLR, 2021.
- [103] Logan Engstrom, Andrew Ilyas, Hadi Salman, Shibani Santurkar, and Dimitris Tsipras. Robustness (python library), 2019. URL <https://github.com/MadryLab/robustness>, 4(4): 4–3, 2019.
- [104] Hadi Salman, Andrew Ilyas, Logan Engstrom, Ashish Kapoor, and Aleksander Madry. Do adversarially robust imagenet models transfer better? *Advances in Neural Information Processing Systems*, 33:3533–3545, 2020.

- [105] Eric Wong, Leslie Rice, and J. Zico Kolter. Fast is better than free: Revisiting adversarial training, 2020.
- [106] Sergey Zagoruyko and Nikos Komodakis. Wide residual networks, 2017.
- [107] Haichao Zhang and Jianyu Wang. Defense against adversarial attacks using feature scattering-based adversarial training. *Advances in Neural Information Processing Systems*, 32, 2019.
- [108] Francesco Croce, Maksym Andriushchenko, Vikash Sehwal, Edoardo Debenedetti, Nicolas Flammarion, Mung Chiang, Prateek Mittal, and Matthias Hein. Robustbench: a standardized adversarial robustness benchmark. *arXiv preprint arXiv:2010.09670*, 2020.
- [109] Jiequan Cui, Shu Liu, Liwei Wang, and Jiaya Jia. Learnable boundary guided adversarial training. In *Proceedings of the IEEE/CVF international conference on computer vision*, pages 15721–15730, 2021.
- [110] Leslie Rice, Eric Wong, and Zico Kolter. Overfitting in adversarially robust deep learning. In *International Conference on Machine Learning*, pages 8093–8104. PMLR, 2020.
- [111] Sylvestre-Alvise Rebuffi, Sven Gowal, Dan A Calian, Florian Stimberg, Olivia Wiles, and Timothy Mann. Fixing data augmentation to improve adversarial robustness. *arXiv preprint arXiv:2103.01946*, 2021.
- [112] Dongxian Wu, Shu-Tao Xia, and Yisen Wang. Adversarial weight perturbation helps robust generalization. *Advances in Neural Information Processing Systems*, 33:2958–2969, 2020.
- [113] Sven Gowal, Chongli Qin, Jonathan Uesato, Timothy Mann, and Pushmeet Kohli. Uncovering the limits of adversarial training against norm-bounded adversarial examples. *arXiv preprint arXiv:2010.03593*, 2020.
- [114] Dan Hendrycks, Kimin Lee, and Mantas Mazeika. Using pre-training can improve model robustness and uncertainty. In *International conference on machine learning*, pages 2712–2721. PMLR, 2019.
- [115] Martin Heusel, Hubert Ramsauer, Thomas Unterthiner, Bernhard Nessler, and Sepp Hochreiter. Gans trained by a two time-scale update rule converge to a local nash equilibrium. *Advances in neural information processing systems*, 30, 2017.

## A Proofs

We can prove the ordering of this Hasse diagram using definition 8. We will first state the following lemmas and use them to prove Theorem 1. We will prove them afterwards.

**Lemma 1.**  $O_{S\&A} \sqsubset O_M$  and  $O_M \not\sqsubset O_{S\&A}$

**Lemma 2.**  $O_L \sqsubset O_S$  and  $O_S \not\sqsubset O_L$

**Lemma 3.**  $O_{SPA} \sqsubset O_A$  and  $O_A \not\sqsubset O_{SPA}$

*Proof: Theorem: 1.* First,  $O_{SPA} \sqsubset O_{L\&SPA}$ ,  $O_S \sqsubset O_{S\&SPA}$ ,  $O_S \sqsubset O_{S\&A}$ ,  $O_A \sqsubset O_{L\&A}$ , and  $O_L \sqsubset O_{L\&A}$  follow directly from definition 9 and part 2(a) of definition 8.

Likewise,  $O_{L\&SPA} \not\sqsubset O_{SPA}$ ,  $O_{S\&SPA} \not\sqsubset O_S$ ,  $O_{S\&A} \not\sqsubset O_S$ ,  $O_{L\&A} \not\sqsubset O_A$ , and  $O_{L\&A} \not\sqsubset O_L$  follow directly from definition 9 and part 2(b) of definition 8.

Using Lemma 2 and part 2(c) of definition 8, we yield that  $O_{L\&A} \sqsubset O_{S\&A}$ ,  $O_{S\&A} \not\sqsubset O_{L\&A}$ ,  $O_{L\&SPA} \sqsubset O_{S\&SPA}$ , and  $O_{S\&SPA} \not\sqsubset O_{L\&SPA}$ .

Using Lemma 3 and part 2(c) of definition 8, we get that  $O_{S\&SPA} \sqsubset O_{S\&A}$  and  $O_{S\&A} \not\sqsubset O_{S\&SPA}$ .

Using all of this in addition to Lemma 1, we get that Theorem 1 holds under the  $\sqsubset$  ordering.  $\square$

We now move on to proving the various Lemmas we used to prove Theorem 1.

*Proof: Lemma 1.* To show  $O_{S\&A} \sqsubset O_M$ , we need to find PPT  $f$  such that,  $\forall a \in \{0, 1\}^*$ ,  $O_{S\&A}(a) = f(O_M(a))$ . Incidentally, we also need that  $State(O_{S\&A}) = f(O_M(a))$  when both oracles are queried the same number of times. We will have two cases, Case 1 where the attacker has unlimited queries, and Case 2 where the attacker is limited.

For the sake of simplicity, we assume that  $a \in I$  (as otherwise they both return  $\square$ ), and we can set  $f$  to return  $\square$  when it receives  $\square$  anyway and  $O_{S\&A}(a) = f(O_M(a))$ .

**Case 1:** Let  $f$  be the following:

- On input  $x \in I$ ,  $f$  receives  $[\theta_M, x] = O_M(x)$ . From  $\theta_M$ , we can construct  $M$  and  $\phi_M$  (by definition of  $\theta_M$ ).
- We can then compute and return  $[M(x), \phi_M, x] = O_{S\&A}(x)$ .

**Case 2:** Let  $f$  be the following and  $k$  the current allowed number of queries left:

- On input  $x \in I$ ,  $f$  receives  $[\theta_M, x] = O_M(x)$ . From  $\theta_M$ , we can construct  $M$  and  $\phi_M$  (by definition of  $\theta_M$ ).
- If  $k = 0$ , return  $[\square, \phi_M, x] = O_{S\&A}(x)$ .
- Else, update  $State(O_M(x))$  to be the function that returns  $[k - 1]$ , return  $[M(x), \phi_M, x] = O_{S\&A}(x)$ .



So we have that  $\forall a \in \{0, 1\}^*$ ,  $O_{S\&A}(a) = f(O_M(a))$ . Hence,  $O_{S\&A} \sqsubset O_M$ .

Now for the opposite,  $O_M \not\sqsubset O_{S\&A}$ . For simplicity's sake, we'll cover only the first case, but the proof also applies to the second case by performing the update to the *State* function as we did above. We'll prove this by contradiction. Given  $O_{S\&A}$ , an attacker can receive  $\phi_M$  and  $M(x)$  for any  $x \in I$ . We are trying to reconstruct  $\theta_M$ . In the case where  $M$  is linear, with enough queries, we can solve the system of linear equations and reconstruct  $\theta_M$ . However, in the case where  $M$  is non-linear, there can be an infinite number of possible viable solutions for any given finite amount of queries, therefore it is impossible to always determine with certainty the exact  $\theta_M$  (although it is possible to approximate it, as model stealing attacks demonstrate). Hence, it is not always possible to reconstruct  $\theta_M$  from  $\phi_M$  and score query-access, meaning that there is no PPT  $f$  s.t.  $\forall a \in \{0, 1\}^*$ ,  $f(O_{S\&A}(a)) = O_M(a)$ .  $\square$

*Proof: Lemma 2.* We will prove Lemma 2 in the same way we proved Lemma 1, i.e.  $\exists f$  such that  $\forall a \in I$ ,  $f(O_S) = O_L$ .

**Case 1. Unlimited queries:** Let  $f$  be the following:

- On input  $x \in \{0, 1\}^*$ , if  $x \notin I$ , then  $f$  receives  $\square$  and return  $\square$ .
- Else, on input  $x \in I$ ,  $f$  receives  $[M(x), x]$  and returns  $[\text{argmax}(M(x)), x] = O_L$ .

**Case 2. Limited queries:** Let  $f$  be the following and  $k$  the current allowed number of queries left:

- On input  $x \in \{0, 1\}^*$ , if  $x \notin I$ , then  $f$  receives  $\square$  and return  $\square$ .
- Else, on input  $x \in I$ ,  $f$  receives  $[M(x), x]$  if  $k > 0$  else it receives  $[\square, x]$ .
- If  $k = 0$ , return  $[\square, x] = O_L$ .
- Else, return  $[\text{argmax}(M(x)), x] = O_L$ .

For the other direction, similarly to Lemma 1, we will prove only the first case as the proof can trivially be extended to the second case. Given  $O_L$ , we want to find a PPT function  $f$  s.t.  $\forall a \in I$ ,  $f(O_L(a)) = O_S(a)$ . We will show that such a function cannot exist. For  $f(O_L(a)) = O_S(a)$  to happen, it means that  $f$  needs to always be able to at least compute the score value of the label itself. It is given no information beyond the label itself for any input  $x \in I$ . Assume the following setup. One party holds two models  $M_1$  and  $M_2$  that make identical score predictions except for one specific input  $x^*$  where  $M_1(x^*) = u$  and  $M_2(x^*) = v$  and  $u \neq v$ , we will also assume that while the score changes when inferring on  $x^*$ , the predicted label remains the same for both. We argue that it would be impossible for the other party that receives only the predicted label to distinguish between both models. This means that there exists at least one instance where there is no PPT function  $f$  s.t.  $\forall a \in I$ ,  $f(O_L(a)) = O_S(a)$ . Therefore, we showed the other direction also holds.

Hence, Lemma 2 holds.  $\square$

In this case, we do not need to modify  $State(O_S)$  as we query  $O_S$  exactly once whenever we query  $O_L$ .

*Proof: Lemma 3.*  $O_{SPA} \sqsubset O_A$  follows from part 1(b) of definition 8 and  $O_{SPA}$ 's definition. For the other direction, since  $O_{SPA}(x) = [\{\phi_0, \phi_1, \dots, \phi_k\}, x]$  for some positive integer  $k$  and where for a uniformly randomly sampled  $i \in [0, 1, \dots, k]$ ,  $\phi_i = \phi_M$ , a PPT function  $f$  would be able to always determine which of the  $k$  elements in the unordered set is the correct architecture. Given that the function is only given the unordered set, it would be akin to being able to always correctly guess a random number, which is not possible. Therefore,  $O_A \not\sqsubset O_{SPA}$  and Lemma 3 holds.  $\square$

*Proof: Theorem 2.* Theorem 2 follows directly from definitions 8 and 9.  $\square$

*Proof: Theorem 3.* By definition, we have the oracles defined by  $O_T$  that are properly defined and ordered under  $\sqsubset$ . It remains to show that  $O_{Train}$  dominates any one of them and none of them dominates  $O_{Train}$ . By how any  $T_i$  is defined, we have that  $Train \in T_i$  for any integer  $i$ . Since  $T_i$  is an unordered set, we can apply part 1(b) of definition 8 to yield that  $\forall i \in \mathbb{Z}$ ,  $O_{T_i} \sqsubset O_{Train}$ . We'll show that  $\forall i \in \mathbb{Z}$ ,  $O_{Train} \not\sqsubset O_{T_i}$  by contradiction. By part 1(c) of definition 8, for any integer  $i$ , there needs to be a PPT function  $f$  such that  $f([T_i, x]) = [Train, x]$  for any  $x \in \{0, 1\}$ . Hence, we need some PPT function that can extract  $Train$  from  $T_i$  (as we know it is in  $T_i$  by definition of  $T_i$ ). However,  $T_i$  is an unordered set and  $f$  only has access to  $T_i$  (and the query itself  $x$  but in this case it should not provide additional information about the ordering of  $T_i$ ). So, for  $f$  to be able to distinguish  $Train$  from any other of the other  $Train'$  functions in  $T_i$  would be equivalent to being able to perfectly guess truly random numbers, which is impossible. Therefore, we have a contradiction and so  $\forall i \in \mathbb{Z}$ ,  $O_{Train} \not\sqsubset O_{T_i}$ .  $\square$

*Proof: Theorem 4.*  $O_{PA} \sqsubset O_{FA}$  follows directly from part 2(c) and 1(b) of definition 8 as well as  $O_{FA}$ 's definition since  $\varrho \in \{\varrho_1, \dots, \varrho_k\}$ .  $O_{FA} \not\sqsubset O_{PA}$  follows from the impossibility of perfectly guessing truly random numbers (since  $i$  s.t.  $\varrho_i = \varrho$  is uniformly randomly sampled) and part 1(c) of definition 8.  $O_{SPD} \sqsubset O_{PA}$  also follows directly from part 2(c) and 1(b) of definition 8 as well as  $O_{SPD}$ 's definition since  $\rho \in \{\rho_1, \dots, \rho_k\}$ .  $O_{PA} \not\sqsubset O_{SPD}$  also follows from the impossibility of perfectly guessing truly random numbers and part 1(c) of definition 8.  $\square$

## B Attack Summary Table

We complete Table 3 with the information from the papers not included in the evaluation in Section 6 with Table 15.

<b>Attack</b> (Targeted)	<b>Model</b>	<b>Data</b>	<b>Train</b>	<b>Metric</b>
ODI [42] (t)	Possible Architectures	Training Data	Training Function	$l_\infty$
GA [37]	Possible Architectures	Training Data	Training Function	$l_\infty$
AI-FGTM [12]	Possible Architectures	Training Data	Training Function	$l_\infty$
F-Attack [35]	Labels	Same Distribution	$\emptyset$	None
Admix (A) [89] (both)	Possible Architectures	Training Data & Same Distribution	Training Function	None
Admix (B) [89] (both)	Architecture	Training Data & Same Distribution	Training Function	None
Admix (C) [89] (both)	Parameters	Same Distribution	Loss Function	None
Shadow [11]	Scores	Other Data	$\emptyset$	None
DAPatch [81]	Parameters	$\emptyset$	$\emptyset$	$l_0$
S <sup>2</sup> I (A) [80] (both)	Possible Architectures	Training Data	Training Function	$l_\infty$
S <sup>2</sup> I (B) [80] (both)	Parameters	$\emptyset$	Loss Function	$l_\infty$
AI-GAN [90] (t)	Parameters	Training Data	$\emptyset$	$l_\infty$
ACA (A) [83]	Possible Architectures	Training Data & Other Data	Training Function	None
ACA (B) [83]	Parameters	Other Data	Loss Function	None
DiffAttack (A) [82]	Possible Architectures	Training Data & Other Data	Training Function	FID [115]
DiffAttack (B) [82]	Parameters	Other Data	Loss Function	FID [115]

Table 15: Attack Summary Table. Supplements Table 3.